

Experimental and Theoretical Investigations of New Dinuclear Palladium Complexes as Precatalysts for the Amination of Aryl Chlorides

Ute Christmann,^{†,§} Dimitrios A. Pantazis,[‡] Jordi Benet-Buchholz,[†]
John E. McGrady,[#] Feliu Maseras,^{†,£} and Ramón Vilar^{*,§}

Contribution from the Department of Chemistry, Imperial College London, South Kensington, London SW7 2AZ, U.K., Institute of Chemical Research of Catalonia (ICIQ), 43007 Tarragona, Spain, Unitat de Química Física, Edifici Cn, Universitat Autònoma de Barcelona, 08193 Bellaterra, Spain, Department of Chemistry, University of York, Heslington, York YO10 5DD, U.K., and WestCHEM, Department of Chemistry, University of Glasgow, G12 8QQ, U.K.

Received November 17, 2005; E-mail: r.vilar@imperial.ac.uk

Abstract: A series of new palladium dinuclear species with general formula $[\text{Pd}_2\text{X}(\mu\text{-X})\{\mu\text{-P}^i\text{Bu}_2(\text{Bph-R})\}]$ ($\text{X} = \text{Cl}, \text{Br}$; Bph = biphenyl; $\text{R} = \text{H}, \text{Me}, \text{NMe}_2$) have been prepared. The two palladium centers in these species are bridged by one of the aromatic rings of the biphenyl group present in the corresponding phosphine. The X-ray crystal structure of one of these complexes has been obtained, providing a clear picture of the bonding pattern. The stability of these dimers in solution is shown to be highly dependent on the nature of the phosphine R group and also on the bridging halide. When $\text{R} = \text{NMe}_2$, the dimers dissociate, yielding the palladium(II) compounds $\text{PdX}_2\{\text{P}^i\text{Bu}_2(\text{BPh-NMe}_2)\}$ ($\text{X} = \text{Cl}, \text{Br}$), and the X-ray crystal structure of one of them ($\text{X} = \text{Br}$) has shown that the biphenyl group from the phosphine interacts directly with the metal center. This interaction seems to play an important role in stabilizing the otherwise coordinatively unsaturated palladium(II) complex. In contrast, when $\text{R} = \text{H}$ or Me , the analogous monomeric palladium(II) complexes are unstable and undergo cyclometalation to generate a palladium(II) dinuclear species in which each of the two phosphines cyclometalates with the palladium centers forming a strained four-membered ring. In addition to their unusual structures, these aryl-bridged dimers have also proven to be excellent precatalysts for the amination of aryl chlorides. To rationalize some of the experimental results, a detailed DFT computational study has been carried out and is presented herein.

Introduction

Palladium-mediated cross-coupling reactions to form C–C, C–N, C–O, and C–S bonds are important organometallic transformations in organic synthesis.^{1–11} These reactions are generally proposed to proceed through a mechanism that involves three distinct steps. Oxidative addition of an aryl halide

to a palladium(0) center (usually stabilized by bulky ligands)^{12–16} is followed by a transmetalation reaction to yield a palladium(II) complex that contains the two moieties to be coupled. The final step is then the reductive elimination of the product with the concomitant regeneration of the active palladium(0) catalyst.

Although the original palladium catalysts for cross-coupling reactions required reactive aryl iodides and bromides as substrates, the past few years have seen important advances in the development of more efficient catalytic systems that can also activate aryl chlorides^{17–25} (which are more readily

[§] Imperial College London.

[†] Institute of Chemical Research of Catalonia.

[£] Universitat Autònoma de Barcelona.

[‡] University of York.

[#] University of Glasgow.

- Hartwig, J. F. *Angew. Chem., Int. Ed.* **1998**, *37*, 2046–2067.
- Tykwinski, R. R. *Angew. Chem., Int. Ed.* **2003**, *42*, 1566–1568.
- Wolfe, J. P.; Wagaw, S.; Marcoux, J.-F.; Buchwald, S. L. *Acc. Chem. Res.* **1998**, *31*, 805–818.
- Miyaura, N.; Suzuki, A. *Chem. Rev.* **1995**, *95*, 2457–2483.
- Cardenas, D. J. *Angew. Chem., Int. Ed.* **2003**, *42*, 384–387.
- Diederich, F.; Stang, P. J., Eds. *Metal-Catalyzed Cross-Coupling Reactions*; Wiley: New York, 1998; Vol. 1, p 517 pp.
- Hiyama, T.; Shirakawa, E. *Handbook of Organopalladium Chemistry for Organic Synthesis*; Wiley: New York, 2002; Vol. 1, pp 285–309.
- Echavarren, A. M.; Cardenas, D. J. *Metal-Catalyzed Cross-Coupling Reactions*, 2nd ed.; Wiley-VCH: Weinheim, Germany, 2004; Vol. 1, pp 1–40.
- Espinete, P.; Echavarren, A. M. *Angew. Chem., Int. Ed.* **2004**, *43*, 4704–4734.
- Beller, M.; Zapf, A. *Handbook of Organopalladium Chemistry for Organic Synthesis*; Wiley: New York, 2002; Vol. 1, pp 1209–1222.
- Frisch, A. C.; Beller, M. *Angew. Chem., Int. Ed.* **2005**, *44*, 674–688.

(12) Hartwig, J. F. *Synlett* **1997**, 329–340.

(13) Hartwig, J. F. *Acc. Chem. Res.* **1998**, *31*, 852–860.

(14) Stambuli, J. P.; Incarvito, C. D.; Buehl, M.; Hartwig, J. F. *J. Am. Chem. Soc.* **2004**, *126*, 1184–1194.

(15) Stambuli, J. P.; Buehl, M.; Hartwig, J. F. *J. Am. Chem. Soc.* **2002**, *124*, 9346–9347.

(16) Aranyos, A.; Old, D. W.; Kiyomori, A.; Wolfe, J. P.; Sadighi, J. P.; Buchwald, S. L. *J. Am. Chem. Soc.* **1999**, *121*, 4369–4378.

(17) Navarro, O.; Kelly, R. A., III; Nolan, S. P. *J. Am. Chem. Soc.* **2003**, *125*, 16194–16195.

(18) Littke, A. F.; Fu, G. C. *Angew. Chem., Int. Ed.* **2002**, *41*, 4176–4211.

(19) Bedford, R. B.; Cazin, C. S. J.; Hazelwood, S. L. *Angew. Chem., Int. Ed.* **2002**, *41*, 4120–4122.

(20) Bedford, R. B.; Hazelwood, S. L.; Limmert, M. E. *Chem. Commun.* **2002**, 2610–2611.

(21) Bedford, R. B.; Welch, S. L. *Chem. Commun.* **2001**, 129–130.

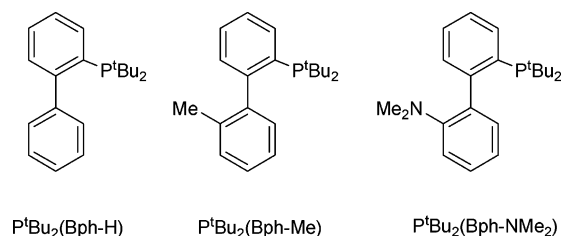
(22) Muci, A. R.; Buchwald, S. L. *Top. Curr. Chem.* **2002**, *219*, 131–209.

available and usually cheaper than their bromide or iodide counterparts). For the less reactive aryl chlorides, the oxidative addition of the substrate is usually the rate-limiting step in the catalytic cycle.²⁶ Consequently, the most recent generation of catalysts is based on palladium complexes containing electron-rich ligands (phosphines or N-heterocyclic carbenes) which facilitate the oxidative addition step. It has been suggested that highly unsaturated [Pd⁰L] species (especially when L is a bulky ligand) are generated in the reaction medium, and that these 12-electron species are responsible for the enhanced activity of these catalytic systems.^{12,13,27–30} In most cases, *standard* palladium sources, such as Pd₂(dba)₃ and Pd(OAc)₂, have been employed to generate the catalytic species in the presence of the corresponding phosphine ligands. More recently, Hartwig^{31,32} and others³³ have shown that the palladium(I) dimer [Pd₂(μ-Br)₂(P^tBu₃)₂], previously synthesized by us,^{34,35} can be used as a novel single-source precatalyst for cross-coupling reactions. High rates for the amination and Suzuki–Miyaura cross-coupling of aryl chlorides and bromides³¹ were observed when this complex was used as precatalyst. The high reactivity of this compound has been attributed to the in situ formation of the monoligated complex [Pd(P^tBu₃)] either by a disproportionation reaction or by direct reduction of the palladium dimer in the presence of substrate and base.

Since the reactivity of palladium(I) dimers is highly dependent on the nature of the coordinated phosphines, the synthesis of a series of dipalladium complexes with phosphines (or other ligands) with a range of different electronic and steric properties is an attractive target. As part of our systematic efforts to prepare novel dinuclear palladium compounds with better catalytic properties for cross-coupling reactions, we have recently turned our attention to sterically demanding biaryl phosphines. Buchwald has shown that several of these phosphines are excellent supporting ligands for the palladium-catalyzed formation of C–C,^{36–39} C–N,^{40–45} and C–O^{22,46–48} bonds using aryl chlorides, bromides, and sulfonates as substrates. The effectiveness

- (23) Zapf, A.; Ehrentraut, A.; Beller, M. *Angew. Chem., Int. Ed.* **2000**, *39*, 4153–4155.
 (24) Zapf, A.; Beller, M. *Chem. Commun.* **2005**, 431–440.
 (25) Grasa, G. A.; Viciu, M. S.; Huang, J.; Nolan, S. P. *J. Org. Chem.* **2001**, *66*, 7729–7737.
 (26) Galardon, E.; Ramdeehul, S.; Brown, J. M.; Cowley, A.; Hii, K. K.; Jutand, A. *Angew. Chem., Int. Ed.* **2002**, *41*, 1760–1763.
 (27) Widenhoefer, R. A.; Buchwald, S. L. *Organometallics* **1996**, *15*, 3534–3542.
 (28) Widenhoefer, R. A.; Buchwald, S. L. *Organometallics* **1996**, *15*, 2755–2763.
 (29) Christmann, U.; Vilar, R. *Angew. Chem., Int. Ed.* **2005**, *44*, 366–374.
 (30) Paul, F.; Patt, J.; Hartwig, J. F. *J. Am. Chem. Soc.* **1994**, *116*, 5969–5970.
 (31) Stambuli, J. P.; Kuwano, R.; Hartwig, J. F. *Angew. Chem., Int. Ed.* **2002**, *41*, 4746–4748.
 (32) Hama, T.; Liu, X.; Culkin, D. A.; Hartwig, J. F. *J. Am. Chem. Soc.* **2003**, *125*, 11176–11177.
 (33) Prashad, M.; Mak, X. Y.; Liu, Y.; Repic, O. *J. Org. Chem.* **2003**, *68*, 1163–1164.
 (34) Vilar, R.; Mingos, D. M. P.; Cardin, C. J. *J. Chem. Soc., Dalton Trans.* **1996**, 4313–4314.
 (35) Dura-Vila, V.; Mingos, D. M. P.; Vilar, R.; White, A. J. P.; Williams, D. J. *J. Organomet. Chem.* **2000**, *600*, 198–205.
 (36) Milne, J. E.; Buchwald, S. L. *J. Am. Chem. Soc.* **2004**, *126*, 13028–13032.
 (37) Barder, T. E.; Buchwald, S. L. *Org. Lett.* **2004**, *6*, 2649–2652.
 (38) Walker, S. D.; Barder, T. E.; Martinelli, J. R.; Buchwald, S. L. *Angew. Chem., Int. Ed.* **2004**, *43*, 1871–1876.
 (39) Nguyen, H. N.; Huang, X.; Buchwald, S. L. *J. Am. Chem. Soc.* **2003**, *125*, 11818–11819.
 (40) Charles, M. D.; Schultz, P.; Buchwald, S. L. *Org. Lett.* **2005**, *7*, 3965–3968.
 (41) Jiang, L.; Buchwald, S. L. *Metal-Catalyzed Cross-Coupling Reactions*, 2nd ed.; Wiley-VCH: Weinheim, Germany, 2004; Vol. 2, pp 699–760.
 (42) Anderson, K. W.; Mendez-Perez, M.; Priego, J.; Buchwald, S. L. *J. Org. Chem.* **2003**, *68*, 9563–9573.
 (43) Huang, X.; Anderson, K. W.; Zim, D.; Jiang, L.; Klapars, A.; Buchwald, S. L. *J. Am. Chem. Soc.* **2003**, *125*, 6653–6655.

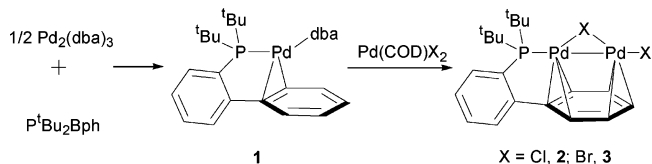
Chart 1



of these systems has been attributed to a combination of electronic and steric properties of the ligands that favor both the oxidative addition and reductive elimination steps in the catalytic cycle.

In a preliminary communication,⁴⁹ we reported the formation of the monophosphine palladium(0) complex Pd(dba){P^tBu₂(Bph-H)} (**1**) (where Bph-H = biphenyl; see Chart 1) which, upon addition of Pd(COD)X₂ (X = Cl, Br), reacts to form the novel dinuclear palladium complexes Pd₂(μ-X)X{μ-P^tBu₂(Bph-H)} (**2**, X = Cl; **3**, X = Br) (see Scheme 1).

Scheme 1



Besides their unusual structural features, these complexes generate catalytically active species for the amination of aryl chlorides and bromides at room temperature. To investigate the synthesis, reactivity, and catalytic properties of this new type of dipalladium compounds in depth, we have carried out the systematic study presented herein. More specifically, we describe the products resulting from the reaction between Pd₂(dba)₃, the biphenyl phosphines P^tBu₂(Bph-R) (R = H, Me, NMe₂; see Chart 1), and Pd(COD)X₂ (X = Cl, Br) and use density functional theory to probe the nature of the metal–ligand interaction. Critically, we show that the nature of the phosphine has an important effect on the stability and reactivity of the products and also on their effectiveness as precatalysts for the room temperature amination of aryl chlorides.

Results and Discussion

Synthesis of the Dinuclear Palladium Complexes Pd₂(μ-X)X{μ-P^tBu₂(Bph-R)} (R = H, Me, NMe₂; X = Cl, Br). On the basis of the recently reported⁴⁹ synthesis of complexes **2** and **3** (see Scheme 1), the analogous methyl-substituted dinuclear compounds Pd₂(μ-X)X{μ-P^tBu₂(Bph-Me)} (X = Cl, **4**; Br, **5**) were successfully prepared from the reaction between Pd₂(dba)₃ and 2 equiv of P^tBu₂(Bph-Me) followed by addition of Pd(COD)X₂ (X = Cl, Br) (see Scheme 2).

- (44) Strieter, E. R.; Blackmond, D. G.; Buchwald, S. L. *J. Am. Chem. Soc.* **2003**, *125*, 13978–13980.
 (45) Zim, D.; Buchwald, S. L. *Org. Lett.* **2003**, *5*, 2413–2415.
 (46) Vorogushin, A. V.; Huang, X.; Buchwald, S. L. *J. Am. Chem. Soc.* **2005**, *127*, 8146–8149.
 (47) Hamada, T.; Chieffi, A.; Ahman, J.; Buchwald, S. L. *J. Am. Chem. Soc.* **2002**, *124*, 1261–1268.
 (48) Kuwabe, S.-i.; Torraza, K. E.; Buchwald, S. L. *J. Am. Chem. Soc.* **2001**, *123*, 12202–12206.
 (49) Christmann, U.; Vilar, R.; White, A. J. P.; Williams, D. J. *Chem. Commun.* **2004**, 1294–1295.

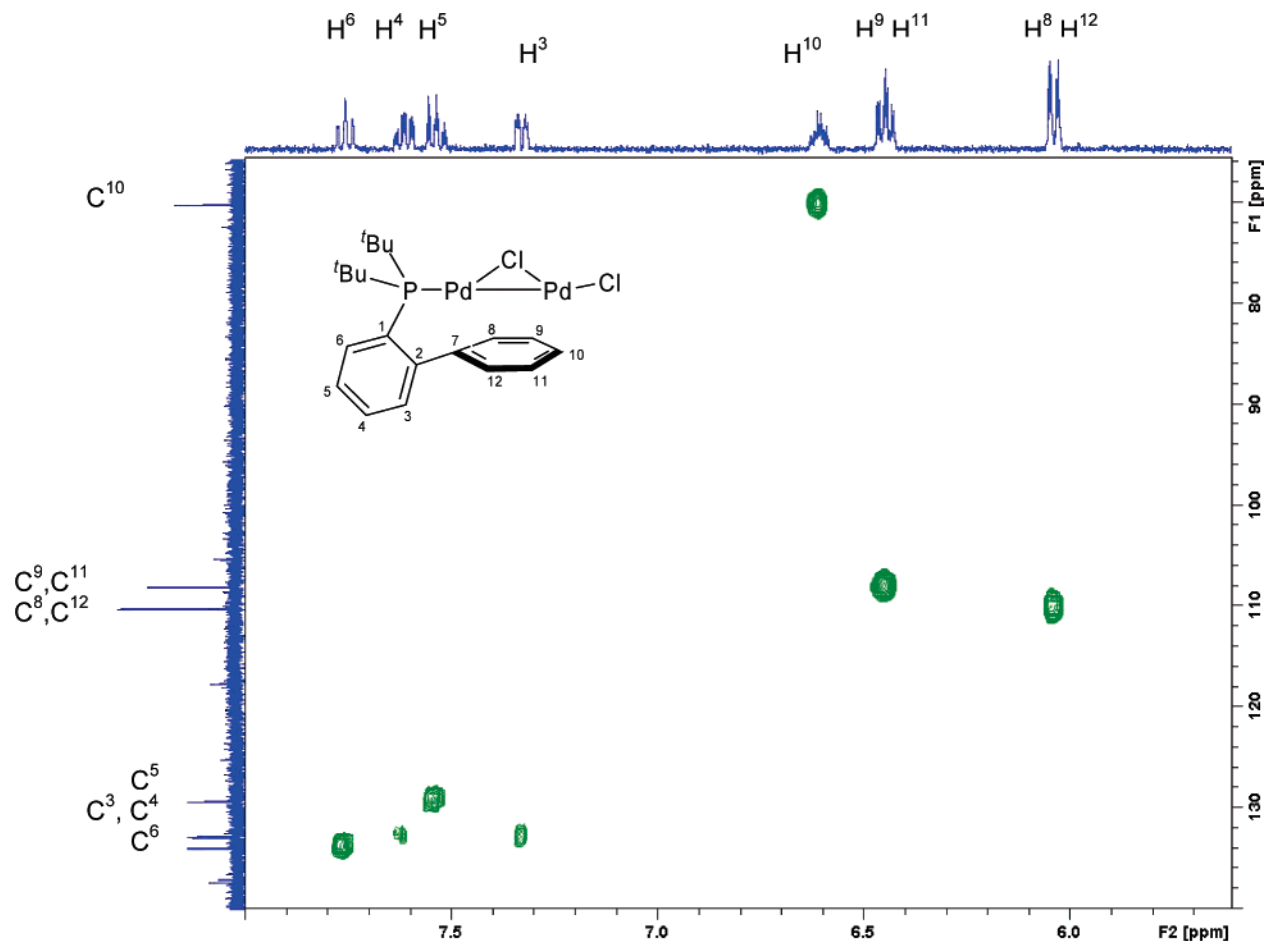
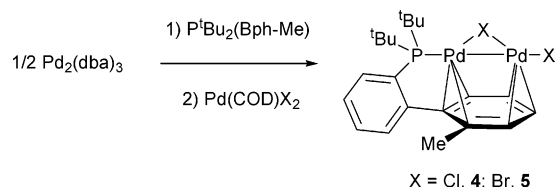


Figure 1. A section of the ^{13}C – ^1H correlation spectrum for **2** showing the cross-peaks for the ^{13}C and ^1H resonances of the biphenyl moiety; the three cross-peaks of the complexed phenyl ring are all shifted to higher field (500 MHz, CD_2Cl_2).

Scheme 2



The products were isolated and characterized on the basis of spectroscopic and analytical techniques. The dinuclear structure of **4** and **5** was supported by elemental analyses and also by ESI mass spectroscopy, which show peaks corresponding to $[\text{M} - \text{X}]^+$ ($\text{X} = \text{Cl}, \text{Br}$). The $^{31}\text{P}\{^1\text{H}\}$ NMR spectra of these complexes show only one singlet each (at 62.1 ppm for **4** and 67.9 ppm for **5**) which is consistent with the proposed formulation. The ^1H and $^{13}\text{C}\{^1\text{H}\}$ NMR spectra of the two complexes are particularly indicative of the presence of a bridging phenyl ring from the biphenyl group since all the aromatic signals corresponding to the ring are shifted to higher field. Analogous shifts have been previously observed in the spectra of the dimeric species **2** and **3**. To assign unambiguously all the resonances, 2D NMR studies were carried out for compounds **2**–**5**. In Figures 1 and 2, the HSQC (^{13}C – ^1H correlation) spectra of **2** (the synthesis and X-ray crystal structure of which we have previously reported⁴⁹) and **4** are shown as examples.

All the hydrogen and carbon atoms associated with the coordinated aromatic ring (C7–C12) are considerably shifted relative to the free phosphine and also to the shifts of the atoms in the aromatic ring (C1–C6) that is not bound directly to the palladium centers. Clearly, the strong interaction between the ring (C7–C12) and the Pd–Pd unit shown previously by an X-ray crystal structure is retained in solution in all four dimers, **2**–**5**.

The dipalladium complex $\text{Pd}_2(\mu\text{-Cl})\text{Cl}\{\text{P}^t\text{Bu}_2(\text{Bph-NMe}_2)\}$ (**6**) was prepared using an analogous procedure to the one described above. The reaction mixture containing $\text{Pd}_2(\text{dba})_3$ and $\text{P}^t\text{Bu}_2(\text{Bph-NMe}_2)$ was stirred for 48 h (until no further free phosphine was observed in the $^{31}\text{P}\{^1\text{H}\}$ NMR spectrum). At this point, solid $\text{Pd}(\text{COD})\text{Cl}_2$ was added, causing a darkening of the solution, and after approximately 1 h a dark precipitate started to form. The reaction mixture was stirred for 2 further hours, after which time it was filtered and crystals of **6** suitable for X-ray crystallography (and spectroscopic characterization) were obtained from the filtrate. The synthesis of the bromide analogue of **6**, $\text{Pd}(\mu\text{-Br})\text{Br}\{\mu\text{-P}^t\text{Bu}_2(\text{Bph-NMe}_2)\}$ (**7**), by a similar protocol was, in contrast, unsuccessful, the reaction instead leading to a monometallic species that will be discussed in a subsequent section.

The X-ray crystallographic study of **6** confirmed it to be a dipalladium complex where the metal centers are bridged by a chloride and by the biphenyl group of $\text{P}^t\text{Bu}_2(\text{Bph-NMe}_2)$. The

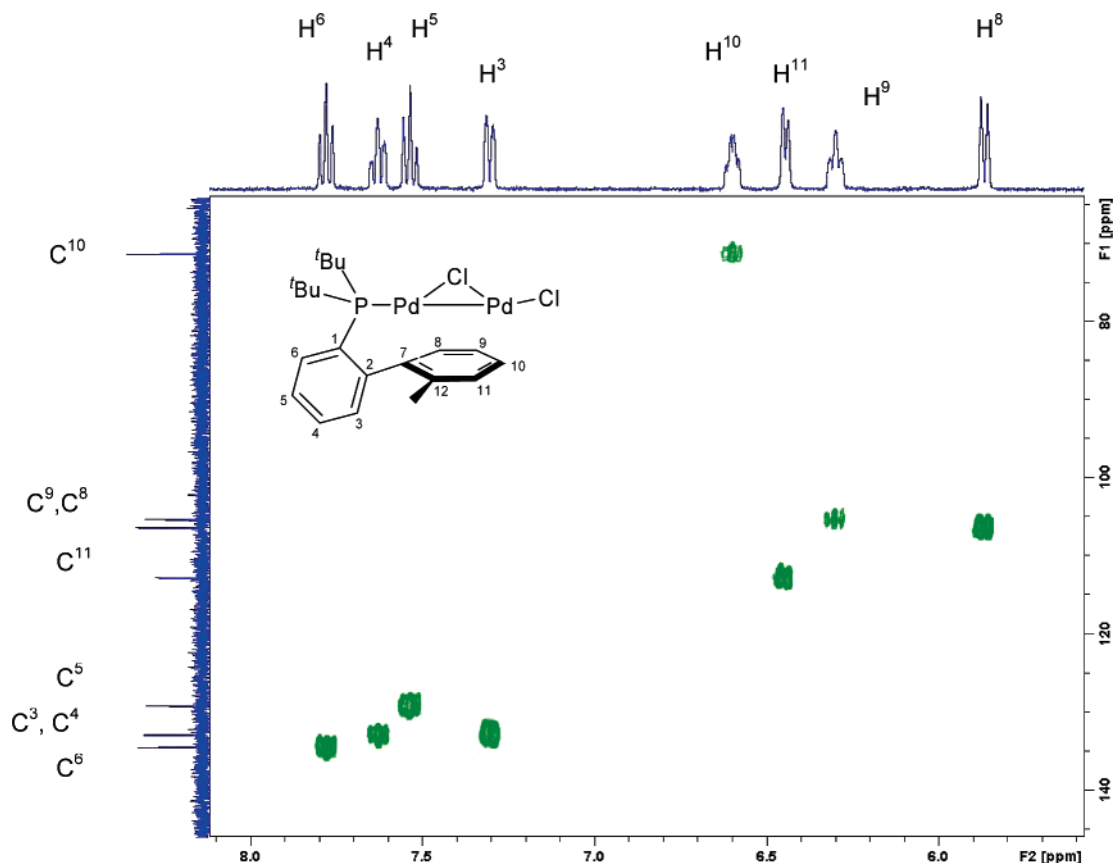


Figure 2. A section of the ^{13}C – ^1H correlation spectrum for **4** showing the cross-peaks for the ^{13}C and ^1H resonances of the biphenyl moiety; the four cross-peaks of the complexed phenyl ring are all shifted to higher field (500 MHz, CD_2Cl_2).

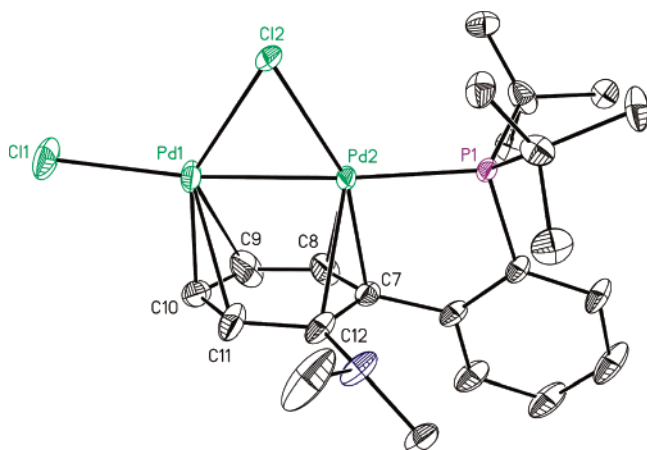


Figure 3. Ortep plot (thermal ellipsoids shown at 50% probability level) of **6**. Hydrogen atoms have been omitted for the sake of clarity. Selected distances (Å): Pd1–Pd2 2.5329(3); Pd1–Cl1 2.3859(8); Pd1–Cl2 2.4391(8); Pd2–Cl2 2.3488(3); Pd2–P1 2.2663(7); Pd1–C9 2.617(5); Pd1–C10 2.099(3); Pd1–C11 2.471(3); Pd2–C8 2.613(4); Pd2–C7 2.136(2); Pd2–C(12) 2.451(3).

molecular structure of **6** (Figure 3) is similar to those of **2** and **3** reported in our preliminary communication, where we described the coordination of the aromatic ring as $\eta^3:\eta^3$.⁴⁹ The coordinated aromatic ring contains a NMe_2 group which lowers the symmetry of the system, making the molecule chiral. Atom C7 has the characteristic pyramidalization detected in the structures of the analogous compounds **2** and **3**, with an angle of 19.5° between the plane of the aromatic ring and the exocyclic bond at C7. All six contacts to the aromatic ring (Pd1–C9,

Pd1–C10, Pd1–C11, Pd2–C8, Pd2–C7, and Pd2–C12) are relatively short, but the plane of the coordinated aromatic ring is not orthogonal to the Pd_2Cl plane. In fact, the contacts from the palladium atoms to the carbon atoms at the aromatic ring are shorter on the side of the NMe_2 group (Pd1–C11 = 2.471(3) Å vs Pd1–C9 = 2.617(5) Å and Pd2–C12 = 2.451(3) Å vs Pd2–C8 = 2.613(4) Å). Moreover, the aromatic ring directly linked to the phosphorus atom does not lie in the Pd_2Cl plane, but is tilted by 10.5° away from the NMe_2 substituent, possibly due to the steric effects of the methyl group.

The solid-state structure of **6** is consistent with the characterization of the bulk sample in solution. Its $^{31}\text{P}\{^1\text{H}\}$ NMR spectrum shows a singlet at 63.6 ppm consistent with the single phosphorus environment present in the complex. The ^1H NMR spectrum of a freshly prepared sample of **6** in CD_2Cl_2 shows again that four of the aromatic protons are considerably shifted to higher field ($\delta_{\text{H}} = 6.50$ – 5.87 ppm) in comparison to the resonances observed for the free phosphine. As was the case for **2**–**5**, this is a clear indication of the coordination of one of the biphenyl aromatic rings to the Pd–Pd unit. Although the compound was fully characterized both in solution and in the solid state, it should be pointed out that if it is left in solution for more than ca. 2 h a second singlet in the $^{31}\text{P}\{^1\text{H}\}$ NMR spectrum appears (at 76.9 ppm), indicating the conversion of the dinuclear compound into a new species (see below for discussion).

In our preliminary communication, we described the coordination of the arene ring in **2** and **3** as $\eta^3:\eta^3$, a relatively uncommon but not unprecedented structural motif.^{50–54} How-

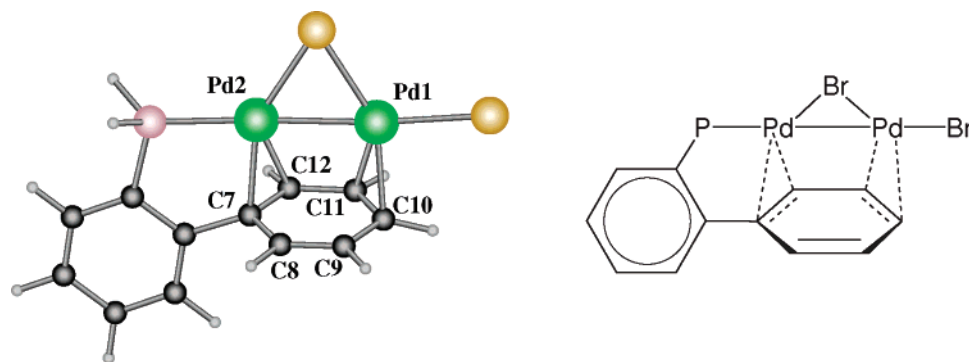


Figure 4. Computed structure for complex **3m** (left) and qualitative description of the bonding of the bridging phenyl to the palladium atoms (right).

ever, the subtle variations in Pd–C bond lengths described above have prompted us to explore the bonding in these systems in greater detail using density functional theory.⁵⁵ The model system chosen for the computational studies was $\text{Pd}_2(\mu\text{-X})\text{X}\{\mu\text{-PH}_2(\text{Bph-R})\}$, where the two *tert*-butyl groups on each phosphine were replaced by hydrogen atoms. The structures of all six possible combinations of X (Br, Cl) and R (H, Me, NMe₂) groups (**2m**–**7m**) were optimized in the gas phase. All optimized geometries share the same principal features, and only a representative example, **3m**, $\text{Pd}_2(\mu\text{-Br})\text{Br}\{\mu\text{-PH}_2(\text{Bph-H})\}$, is shown in Figure 4, which also introduces the atom numbering that will be used in the subsequent discussion.

The main features of the computed geometry of **3m**, most notably the Pd–Pd (2.578 Å cf. experimental value of 2.563 Å) and Pd–($\mu\text{-Br}$) distances (2.485 and 2.508 Å cf. experimental values of 2.462, 2.563 Å), are in reasonable agreement with the X-ray structure of **3**. There are, however, some differences related to the arrangement of the bridging phenyl group which we consider significant. As in the X-ray crystal structure, the plane of the phenyl group is almost perfectly parallel to the Pd–Pd axis, with computed Pd2–C7 and Pd1–C10 distances of 2.165 and 2.148 Å, respectively. This phenyl group plane is not, however, perpendicular to the Pd–Br–Pd plane, but instead is quite tilted, with C12 and C11 much closer to their respective palladium centers (Pd2–C12 = 2.371 Å; Pd1–C11 = 2.252 Å) than C9 and C8 (Pd2–C8 = 2.744 Å; Pd1–C9 = 2.790 Å). The differences in Pd–C distances of 0.373 and 0.538 Å are significantly larger than those in the X-ray structure (0.297 and 0.102 Å), suggesting that the degree of tilt is overestimated in the calculation. The long computed Pd1–C9 and Pd2–C8 distances (>2.7 Å) have led us to re-examine the η^3 : η^3 description proposed previously. The trends in C–C distances are also interesting in this regard: C9–C8 is only 1.371 Å, which is the shortest C–C distance in the phenyl ring by more than 0.04 Å, the other five distances being 1.428, 1.416, 1.421, 1.436, and 1.450 Å for C7–C12, C12–C11, C11–C10, C10–C9, and C7–C8, respectively. The short C9–C8 distance

suggests significant double bond character and a partial breaking of the aromaticity of the phenyl ring as a result of its interaction with the palladium centers. In isolation, the loss of aromaticity would, of course, also lead to a contraction of C7–C12 and C11–C10, but these two are the bonds interacting most strongly with the palladium atoms, and back-donation from the metals masks the expected lengthening. We therefore suggest that the most appropriate description for the bonding in compound **3m**, $[\text{Pd}_2\text{Br}(\mu\text{-Br})\{\mu\text{-PH}_2(\text{Bph-H})\}]$, is the μ - η^2 : η^2 mode presented in the right-hand side of Figure 4, with η^2 interactions between Pd2, C7 and C12 and Pd1, C11 and C10, giving the formal 16-electron count expected for an approximately square planar coordination sphere.

It is possible that the discrepancy between crystallographic and computed structures could be an artifact associated with the replacement of the phosphine *tert*-butyl groups by less bulky and less electron-donating hydrogen atoms in our computational model. We have checked this possibility by carrying out two additional calculations designed to probe the electronic and steric influence of the phosphine substituents. To introduce the electronic effects of the substituents, we carried out a geometry optimization on the model system **3m'**, $\text{Pd}_2(\mu\text{-Br})\text{Br}\{\mu\text{-PMe}_2(\text{Bph-H})\}$, where the *tert*-butyl groups have been replaced by methyl groups instead of hydrogens. The resulting geometry was very similar to that obtained for **3m**; in particular, the tilt of the phenyl ring was conserved, with two short (Pd2–C12, Pd1–C11, 2.359 and 2.261 Å, respectively) and two long (Pd2–C8, Pd1–C9, 2.738 and 2.787 Å, respectively) Pd–C distances. The steric influence of the phosphine substituent was then modeled through an ONIOM calculation [ONIOM(mPW1PW91:UFF)] on the real system **3**, with the *tert*-butyl substituents included in the MM region. Results were again similar to those of the calculation on **3m**, with Pd2–C12, Pd1–C11 distances shorter than 2.4 Å and Pd2–C8, Pd1–C9 distances longer than 2.75 Å. These additional calculations convince us that the tilting of the phenyl group is not a computational artifact, and the fact that the tilting is much less exaggerated in the X-ray structure (leading to our previous η^3 : η^3 description) is most probably due to disorder between the structure shown in Figure 4 and its enantiomer, where the C8–C9 bond is closer to the metal. The barrier separating the enantiomers is very small, and rapid interconversion between the two in solution would mean that the asymmetric coordination of the arene ring is not apparent in the NMR data.

As noted above, the computed structures for **2m**, **4m**, **5m**, **6m**, and **7m** are very similar to those of **3m**, and their structures

(50) Allegra, G.; Tettamanti Casagrande, G.; Immirzi, A.; Porri, L.; Vitulli, G. *J. Am. Chem. Soc.* **1970**, *92*, 289–293.

(51) Kannan, S.; James, A. J.; Sharp, P. R. *J. Am. Chem. Soc.* **1998**, *120*, 215–216.

(52) Dupont, J.; Pfeffer, M.; Rotteveel, M. A.; De Cian, A.; Fischer, J. *Organometallics* **1989**, *8*, 1116–1118.

(53) Sommovigo, M.; Pasquali, M.; Leoni, P.; Braga, D.; Sabatino, P. *Chem. Ber.* **1991**, *124*, 97–99.

(54) Retboll, M.; Edwards, A. J.; Rae, A. D.; Willis, A. C.; Bennett, M. A.; Wenger, E. *J. Am. Chem. Soc.* **2002**, *124*, 8348–8360.

(55) Computational studies on related systems have been recently reported: Barder, T. E.; Walker, S. D.; Martinelli, J. R.; Buchwald, S. L. *J. Am. Chem. Soc.* **2005**, *127*, 4685–4696.

and energies are collected in the Supporting Information. The only qualitative difference with the discussion above arises from the presence of the Me or NMe₂ substituents which leads to two distinct minima, one where the uncoordinated double bond carries the substituent, the other where it does not. For **5m** (X = Br and R = Me), these two local minima, **5m-a** and **5m-b**, are only 0.8 kcal/mol apart. The situation with R = NMe₂ is even more complex because different orientations of the lone pair on the nitrogen are possible. In fact, for system **6m** (X = Cl and R = NMe₂), three distinct local minima were located, all of which lie within 3.5 kcal/mol of each other. The most stable of the three is not the one that most closely resembles the X-ray structure for **6**, but given the small energy differences involved, the solid-state structure is probably strongly influenced by crystal packing effects. The conformation of the absolute minimum is, however, probably of little chemical relevance because the different isomers are likely to be involved in fast equilibria.

Dissociation and Rearrangement of the Dinuclear Palladium Complexes Pd₂(μ-X)X{μ-P'Bu₂(Bph-R)} (R = H, Me, NMe₂; X = Cl, Br) in Solution. We noted in the previous section that attempted synthesis of the bromide compound Pd(μ-Br)Br{μ-P'Bu₂(Bph-NMe₂)} (**7**) was unsuccessful. In fact, when a mixture of Pd₂(dba)₃ and P'Bu₂(Bph-NMe₂) (which had been stirred for 48 h) was reacted with Pd(COD)Br₂, the formation of a dark solid was observed within 1 h (along with some palladium metal formed as a mirror in the reaction vessel). The crude solid was isolated by filtration, and a dark blue compound was extracted using dichloromethane. After filtering this solution, the dichloromethane was evaporated under reduced pressure to give a dark blue solid, which was further purified by column chromatography to yield a product that was formulated, based on spectroscopic and structural characterization, as the new palladium(II) compound PdBr₂{P'Bu₂(BPh-NMe₂)} (**8**) (see Scheme 3).

The structure of **8** was confirmed by X-ray single-crystal structural analysis (see Figure 5). The compound crystallizes in the *Pnma* space group with a C_s pseudo-symmetry plane defined by the approximately square planar coordination sphere around the palladium(II) center. The *tert*-butyl groups and the aromatic ring containing the NMe₂ group are disordered on both sides of this plane. A structure refinement at lower symmetries was also tested (*Pna*2₁), leading to similar *R* values and a strong correlation at the refinement of the atoms. The most significant feature of this structure is the interaction between the palladium center and the biphenyl ipso carbon (C7). The presence of this type of Pd–C_{ipso} bond in palladium(II) complexes is unusual but not unknown (see for example the work by Kocovsky,⁵⁶ and by Campora and Carmona^{57,58}). The Pd–C_{ipso} bond length of 2.191(3) Å is similar to that reported by Kocovsky (2.187 Å)⁵⁶ but shorter than those described previously by Carmona and Campora (2.343(6) and 2.39(1) Å).^{57,58} It is likely that this short Pd–C_{ipso} distance is playing an important role in stabilizing the otherwise coordinatively unsaturated complex. As expected, the Pd–C_{ipso} interaction causes a pyramidalization at C7 and

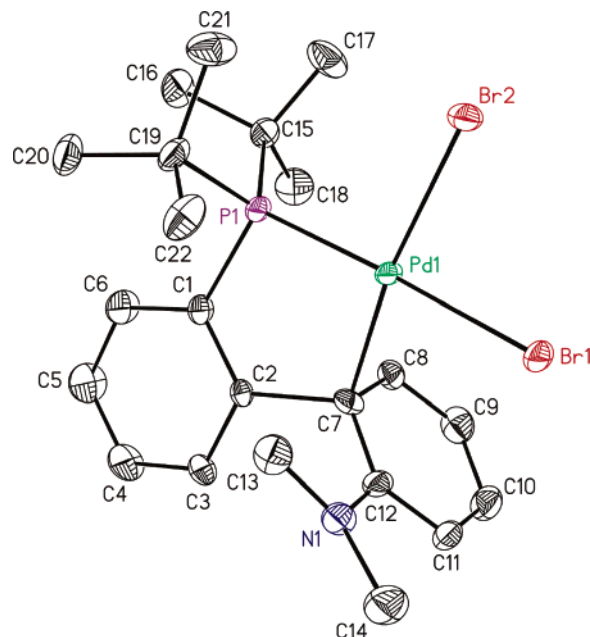


Figure 5. Ortep plot (thermal ellipsoids shown at 50% probability level) of **8**. Hydrogen atoms have been omitted for the sake of clarity. Selected distances (Å) and angles (deg): Pd1–P1 2.2886(6); Pd1–C7 2.191(3); Pd1–Br1 2.4870(3); Pd1–Br2 2.4728(4); C1–C2 1.393(4); C2–C7 1.531(4); C7–C8 1.469(6); C7–C12 1.435(4); P1–Pd1–C7 85.52(9); Pd1–C7–C2 109.39(19); C1–C2–C7 120.8(2); P1–C1–C2 116.31(17); Br1–Pd1–Br2 86.606(12); C2–C7–C10 134.

also an elongation of the aromatic bonds C7–C8 and C7–C12 to 1.469(6) and 1.435(4) Å, respectively. The single bond C7(sp²)–C2(sp²) is also significantly elongated to 1.531(4) Å. As a consequence of the strain in the system, C7 shows a deviation of approximately 0.11 Å from the mirror plane that defines the C_s pseudo-symmetry. The spectroscopic characterization in solution of a bulk sample of **8** is consistent with the structure found by X-ray crystallography.

We also noted in the previous section that the dipalladium compound **6** is prone to decomposition in solution, and the elucidation of the structure of **8** led us to speculate that the decomposition product of **6** could be its chloride analogue. Consequently, a sample of **6** was dissolved in CD₂Cl₂, and the solution was monitored by ³¹P{¹H} NMR spectroscopy for 24 h. After approximately 2 h, a new resonance appeared in the spectrum of this solution (at δ_P = 76.9 ppm), while the resonance associated with the original dipalladium complex **6** (δ_P = 63.6 ppm) slowly decreased in intensity. After 12 h, the ³¹P{¹H} NMR spectrum indicated that **6** had completely converted into the new product with δ_P = 76.9 ppm. No further changes were observed after an additional 24 h of stirring. The compound associated with the δ_P = 76.9 ppm signal was isolated and, on the basis of spectroscopic characterization, formulated as the palladium(II) compound PdCl₂{P'Bu₂(Bph-NMe₂)} (**9**) (see below for synthesis of the same complex via a different route). Although no structural characterization of this compound was carried out, we anticipate that a Pd–C_{ipso} interaction similar to that in **8** stabilizes the otherwise coordinatively unsaturated palladium(II) complex. The ¹³C{¹H} NMR spectrum of this compound is certainly consistent with the presence of such an interaction since the chemical shift of the C_{ipso} appears considerably shifted at δ_C = 86.5 ppm (compared to 117.4 ppm for the free phosphine).

- (56) Kocovsky, P.; Vyskocil, S.; Cisarova, I.; Sejbál, J.; Tislerova, I.; Smrcina, M.; Lloyd-Jones, G. C.; Stephen, S. C.; Butts, C. P.; Murray, M.; Langer, V. *J. Am. Chem. Soc.* **1999**, *121*, 7714–7715.
- (57) Campora, J.; Gutierrez-Puebla, E.; Lopez, J. A.; Monge, A.; Palma, P.; Del Río, D.; Carmona, E. *Angew. Chem., Int. Ed.* **2001**, *40*, 3641–3644.
- (58) Campora, J.; Lopez, J. A.; Palma, P.; Valerga, P.; Spillner, E.; Carmona, E. *Angew. Chem., Int. Ed.* **1999**, *38*, 147–151.

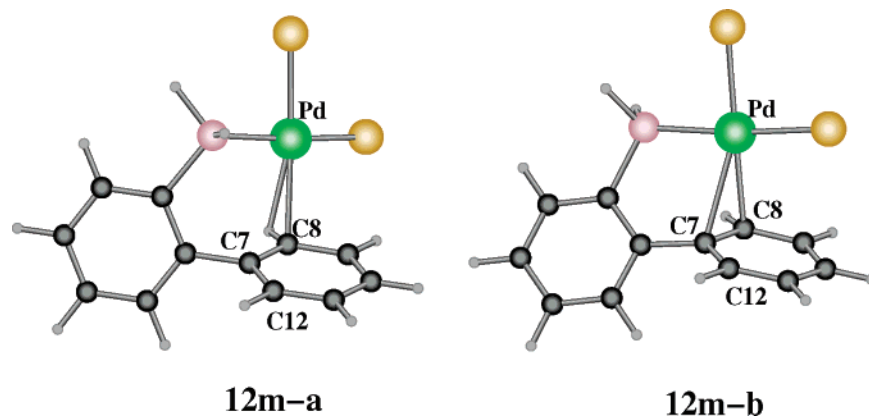


Figure 6. Computed structures for complexes **12m-a** (left) and **12m-b** (right).

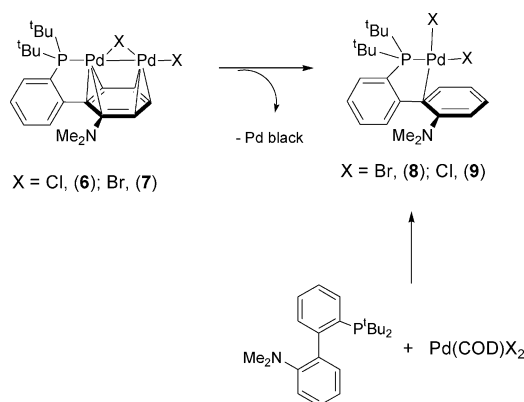
Once the decomposition path of **6** in solution was established, it was of considerable interest to know whether the other dinuclear compounds, **2–5**, would behave in an analogous way if left in solution over extended periods of time. When a sample of **4** was dissolved in CD_2Cl_2 , a new signal at 75.6 ppm started to appear after approximately 10 h, while the resonance associated with **4** ($\delta_{\text{P}} = 62.1$ ppm) decreased in intensity, and palladium black was formed in the NMR tube. The chemical shift of the new species (75.6 ppm) is in the same region of the spectrum as those observed for **8** and **9**, leading us to formulate it as the palladium(II) complex $\text{PdCl}_2\{\mu\text{-P}^t\text{Bu}_2(\text{Bph-Me})\}$ (**10**).

To establish whether the palladium(II) compounds **8** and **9** could be prepared directly from a palladium(II) source and the corresponding phosphine, the reactions between $\text{Pd}(\text{COD})\text{X}_2$ ($\text{X} = \text{Cl}, \text{Br}$) and $\text{P}^t\text{Bu}_2(\text{Bph-NMe}_2)$ were carried out. The reactions were monitored by $^{31}\text{P}\{^1\text{H}\}$ NMR spectroscopy which indicated that, in each case, the only product formed was indeed the corresponding $\text{PdX}_2\{\mu\text{-P}^t\text{Bu}_2(\text{Bph-NMe}_2)\}$ compound ($\text{X} = \text{Br}$, **8**; $\text{X} = \text{Cl}$, **9**). The products were isolated in high yields and fully characterized, confirming that they could be obtained either through decomposition of the dinuclear species or directly from $\text{Pd}(\text{COD})\text{X}_2$ (see Scheme 3). The reactions between $\text{Pd}(\text{COD})\text{Cl}_2$ and $\text{P}^t\text{Bu}_2(\text{Bph-Me})$ were also carried out, yielding the expected $\text{PdCl}_2\{\mu\text{-P}^t\text{Bu}_2(\text{Bph-Me})\}$ compound (**10**). However, as will be discussed in the following section, this complex converted to yet another product when left in solution for longer periods of time (ca. 12 h) (see following section for detailed discussion).

The relatively unusual η^1 coordination mode of the arene in **8** (and, presumably, also **9**) raises questions concerning the nature of the metal–arene interaction and the role of these interactions in controlling the stability of potential intermediates in the catalytic cycle. To compare the relative stability of this type of compound with different combinations of halide and phosphine, computational studies were carried out on the compounds with all possible combinations of X and R groups (although only the first three have been isolated experimentally). The following model systems, $\text{PdX}_2(\text{PH}_2\text{Bph-R})$ **8m** ($\text{X} = \text{Br}$, $\text{R} = \text{NMe}_2$), **9m** ($\text{X} = \text{Cl}$, $\text{R} = \text{NMe}_2$), **10m** ($\text{X} = \text{Br}$, $\text{R} = \text{Me}$), **11m** ($\text{X} = \text{Cl}$, $\text{R} = \text{Me}$), **12m** ($\text{X} = \text{Br}$, $\text{R} = \text{H}$), and **13m** ($\text{X} = \text{Cl}$, $\text{R} = \text{H}$), were studied.

We first present the results for **12m** (with $\text{X} = \text{Br}$ and $\text{R} = \text{H}$), where the absence of a Me or NMe_2 substituent simplifies the discussion. Two different isomers of **12m** were optimized, **12m-a** and **12m-b**, both of which are presented in Figure 6.

Scheme 3



In the less stable of the two isomers, **12m-b**, the coordination of the arene ring is rather similar to that in the dinuclear species **3m**, with two short Pd–C distances, Pd–C7 and Pd–C8, of 2.614 and 2.425 Å, respectively, consistent with an η^2 coordination mode, albeit a highly distorted one. In contrast, there is only one short Pd–C contact, Pd–C8 (2.415 Å), in the more stable isomer **12m-a**, the next nearest carbon being C12, 2.958 Å away. The highly asymmetric coordination mode in **12m-a** could be described as η^1 , although the rather short Pd–H distance indicates some degree of C–H agostic character. Consistent with this, the C8–H bond length of 1.098 Å is significantly longer than the other four C–H bonds in the phenyl ring, which all fall between 1.083 and 1.085 Å. Our previous experience suggests that a lengthening of more than 0.01 Å in such a strong bond is indicative of an agostic bond. Calculations on **8m**, **9m**, **10m**, **11m**, and **13m** all follow the same pattern, with two distinct local minima present in each case, one C–H agostic, the other featuring an $\eta^2\text{-C}=\text{C}$ coordination mode. It is rather unusual for a C–H agostic bond to compete with an $\eta^2\text{-C}=\text{C}$ interaction, but in this case, the chelating nature of the ligand prevents the arene ring from adopting an orientation that optimizes the latter. This is most clearly illustrated by a further calculation on the model system $\text{PdBr}_2(\text{PH}_3)(\text{C}_6\text{H}_6)$, where the phenyl group linking the phosphorus center and the coordinating arene ring has been removed. In this case, where the benzene ring is completely unconstrained, it rotates by approximately 30° , such that the C7–C8 vector is perpendicular to the P–Pd–Br plane. The overall effect of the chelating ligand is therefore to destabilize the $\eta^2\text{-C}=\text{C}$ interaction and cause a distinct slippage toward a highly asymmetric η^2 , or even η^1 ,

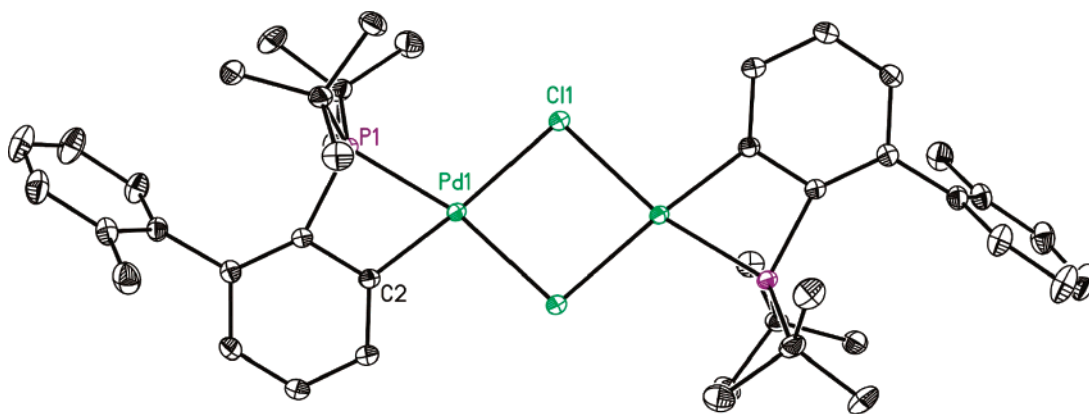


Figure 7. Ortep plot (thermal ellipsoids shown at 50% probability level) of **14**. Hydrogen atoms have been omitted for the sake of clarity. Selected distances (Å) and angles (deg): Pd1–P1 2.2392(3); Pd1–C2 1.9868(12); Pd1–Cl1 2.4668(1); Pd1–Cl1A 2.4261(3); C1–C2 1.4047(15); P1–Pd1–C2 68.69(3); P1–C1–C2 95.07(8); Pd1–P1–C1 86.29(4); Pd1–C2–C1 109.57(9); P1–Pd1–Cl1 106.792(11); C2–Pd1–Cl1A 99.02(3); Cl1–Pd1–Cl1A 85.463(11).

mode. Mealli⁵⁹ and Barder⁶⁰ have recently discussed similar features in the bonding in constrained Pd–arene complexes.

The relatively weak interaction between the metal and the arene ring in both **12m-a** and **12m-b** prompted us to reintroduce the *tert*-butyl groups on phosphorus into our computational model, as their steric influence may be of similar magnitude to the strength of the metal–arene bond. This possibility is most apparent in the structure of **12m-a**, where the interaction between Pd and the C8–H bond introduces a torsion about the P–C bond and forces one of the hydrogen atoms on phosphorus to point directly toward the hydrogen bound to the *ortho* carbon of the phenyl group. We have therefore carried out ONIOM calculations on the complete complex **12**, PdBr₂(P^{*t*}Bu₂Bph-H), incorporating the *tert*-butyl groups in the MM partition. Two different isomers could again be located, **12-a** and **12-b**, separated by only 0.4 kcal/mol, but both now feature relatively symmetric η^2 -C=C coordination and differ only in the conformational arrangement of the *tert*-butyl groups. The local minima corresponding to agostic C–H species therefore disappear when the bulky phosphine substituents are included, and ONIOM calculations on systems **8**–**13** confirm this to be the case in all the systems. As anticipated above, the disappearance of the agostic minima can be traced to the steric clash between the *tert*-butyl groups and the *ortho* C–H of the ring bound to phosphorus. The bulky substituents on the phosphorus force the *ortho* C–H group to bisect the C–P–C angle, rather than pointing directly at one of the substituents on P, as was the case in **12m-a**. This, in turn, forces the remote arene ring to adopt a more symmetric position with respect to the palladium center and hence favors the distorted η^2 -C=C coordination mode.

Perhaps the most striking aspect of the ONIOM calculation on complex **8** (X = Br, R = NMe₂) is that the most stable isomer, **8-a**, features a highly asymmetric coordination mode, which could be described either as η^1 or as distorted η^2 , precisely as is observed in the X-ray structure. The computed Pd–C7 distance is 2.439 Å, significantly shorter than the Pd–C12 and Pd–C8 distances of 2.777 and the 2.974 Å. The calculated Pd–C7 distance is rather longer than the X-ray value of 2.191 Å, but the origin of the discrepancy may again lie in the disorder

of the aromatic group noted in the X-ray study. A comparison of the computed structures with (**8**) and without (**8m**) the *tert*-butyl groups clearly indicates that the unusual coordination mode is again a result of a compromise between the steric bulk of the phosphine substituents, favoring a symmetric orientation of the arene ring and hence η^1 coordination, and the intrinsic electronic driving force favoring the η^2 alternative. The fact that the chelating nature of the ligand prevents the system from optimizing the η^2 -C=C interaction makes the potential energy surface for ring slippage very soft and hence allows steric factors to play a dominant role.

Synthesis of the Cyclopalladated 14. As noted in the previous section, when a sample of **10** was left in solution for more than 12 h, the ³¹P{¹H} NMR spectrum indicated that it was fully converted to yet another product, **14**, with $\delta_P = -13.1$ ppm, which was isolated from the reaction mixture and fully characterized via spectroscopic, structural, and analytical techniques. It has previously been reported that cyclometalated phosphines featuring four-membered rings show very different ³¹P NMR chemical shifts compared to their analogous noncyclometalated counterparts.⁶¹ On the basis of the unusually high field resonance for **14**, the complex was therefore formulated as a cyclometalated dipalladium(II) compound (see Scheme 4) in which intramolecular activation of an *ortho* C–H of the P^{*t*}Bu₂(Bph-Me) phosphine generates a strained four-member ring.

The proposed structure of **14** was unambiguously established by a single-crystal X-ray structural analysis, which reveals a dipalladium(II) species bridged by two chlorides, each palladium center being part of a cyclometalated four-membered ring (Figure 7). The compound crystallizes as a chloroform solvate with *C*_i molecular symmetry, with the phosphorus atoms located in a *trans* position with respect to each other. The Pd1–C2 distance (1.9868(12) Å) is within the range of values found in similar four-membered complexes with a sp²-hybridized carbon. As a result of the strain produced by the unusual four-membered ring (atoms Pd1–P1–C1–C2), the angle P1–Pd1–C2 is reduced to 68.69(3)° (compared to average values of 67.8° in similar monomeric systems with a four-membered azapalladacycle).^{62,63} The other endocyclic angles in the four-membered

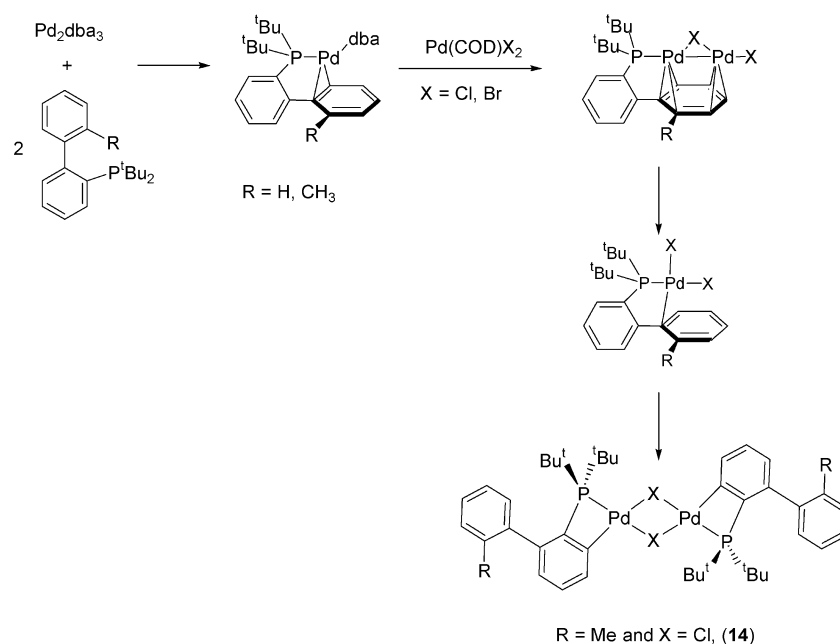
(59) Catellani, M.; Mealli, C.; Motti, E.; Paoli, P.; Perez-Carreño, E.; Pregosin, P. S. *J. Am. Chem. Soc.* **2002**, *124*, 4336–4346.

(60) Barder, T. E. *J. Am. Chem. Soc.* **2006**, *128*, 898–904.

(61) Garrou, P. E. *Chem. Rev.* **1981**, *81*, 229–266.

(62) Sole, D.; Vallverdu, L.; Solans, X.; Font-Bardia, M.; Bonjoch, J. *Organometallics* **2004**, *23*, 1438–1447.

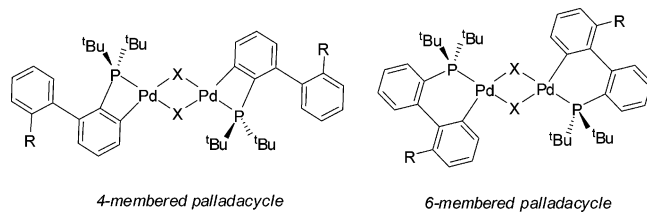
Scheme 4



ring are also smaller than expected ($\text{Pd1-P1-C1} = 86.29(4)^\circ$; $\text{P1-C1-C2} = 95.07(8)^\circ$; and $\text{Pd1-C2-C1} = 109.57(9)^\circ$). The difference between the P1-Pd1-C11 ($106.792(11)^\circ$) and C2-Pd1-C11A ($99.02(3)^\circ$) angles is probably due to the repulsive steric effects of the bulky *tert*-butyl group. As the computational studies reported below demonstrate, the steric bulk of these groups plays a key role in driving the formation of the four-membered ring rather than its six-membered analogue.

Once the conversion of **4** to the cyclometalated product **14** (via **10**) was confirmed, the analogous process for **2**, **3**, and **5** was investigated by $^{31}\text{P}\{^1\text{H}\}$ NMR spectroscopy. In all three cases, the biphenyl-bridged dipalladium compounds convert to the corresponding cyclometalated products (all of which appear at a chemical shift between -14.0 and -18.7 ppm) via a process that involves initial dissociation of the dimer into species analogous to the palladium(II) compound **8**. The conversion times are highly dependent on the coordinated halide and phosphine and on the solvent used; all compounds dissociate and cyclometalate more rapidly in CH_2Cl_2 than in THF. The least stable of the four compounds proved to be $\text{Pd}(\mu\text{-Br})\text{Br}\{\mu\text{-P}^t\text{Bu}_2(\text{Bph-H})\}$ (**3**), which starts to dissociate in THF after ca. 3.5 h and eventually converts to the corresponding four-membered cyclometalated product. The other three compounds remain stable in THF solution for at least 3 h.

Scheme 5



The formation of the four-membered metallacycle in **14** was rather unexpected because an alternative six-membered ring,

which we might anticipate to be more stable, was also accessible through activation of a C–H bond on the remote arene ring (see Scheme 5). To probe the origin of the regioselectivity of the cyclometalation reaction, we have surveyed the potential energy surface for the model complex **14m**, $[\text{Pd}(\mu\text{-Cl})(\text{PH}_2\text{-Bph})_2]$. In this dimeric species, the *tert*-butyl groups have again been replaced by hydrogens, as has the methyl group on the arene ring in **14**. Geometry optimizations confirmed the presence of two distinct isomers, one with four-membered rings, labeled as **14m-4r**, the other with two six-membered rings, labeled as **14m-6r**. The geometry of **14m-4r** is reasonably similar to the X-ray structure of **14**, with a diamond-shaped $\text{Pd}(\mu\text{-Cl})_2\text{Pd}$ core and Pd–Cl distances of 2.463 and 2.394 Å (cf. the experimental values of 2.4668(1) and 2.4261(3) Å). The alternative structure, **14m-6r**, also features a diamond-shaped core, albeit rather more puckered than that in **14m-4r**. The most conspicuous feature of the comparison of the two isomers is, however, their energies: **14m-6r** is 23.2 kcal/mol *more* stable than **14m-4r**, the experimentally observed isomer. In light of our previous results, it seemed likely that the steric bulk of the *tert*-butyl groups may play a significant role in determining the relative stabilities of the products; in particular, the introduction of the remote arene group into the metal coordination sphere in **14-6r** necessarily increases the steric crowding in this case. Steric effects will be sensitive to the nature of the phosphine substituents, so a new set of calculations with the ONIOM method were carried out on system **14**, where the four *tert*-butyl substituents on the phosphines are introduced at the molecular mechanics (UFF) level. We have located a number of different local minima for these systems; the ones we have selected for analysis are **14-4r** and **14-6r**, shown in Figure 8. The geometries are similar to those from the corresponding **14m** model systems, but their relative energies are quite different; the inclusion of the *tert*-butyl groups destabilizes **14-6r** relative to **14-4r**, and the two are now almost isoenergetic, **14-4r** lying only 0.3 kcal/mol above **14-6r**. It is thus evident that steric effects strongly favor the structure with the four-membered rings. The reason for this can be clearly seen in Figure 8, where

(63) Sole, D.; Vallverdu, L.; Solans, X.; Font-Bardia, M.; Bonjoch, J. *J. Am. Chem. Soc.* **2003**, *125*, 1587–1594.

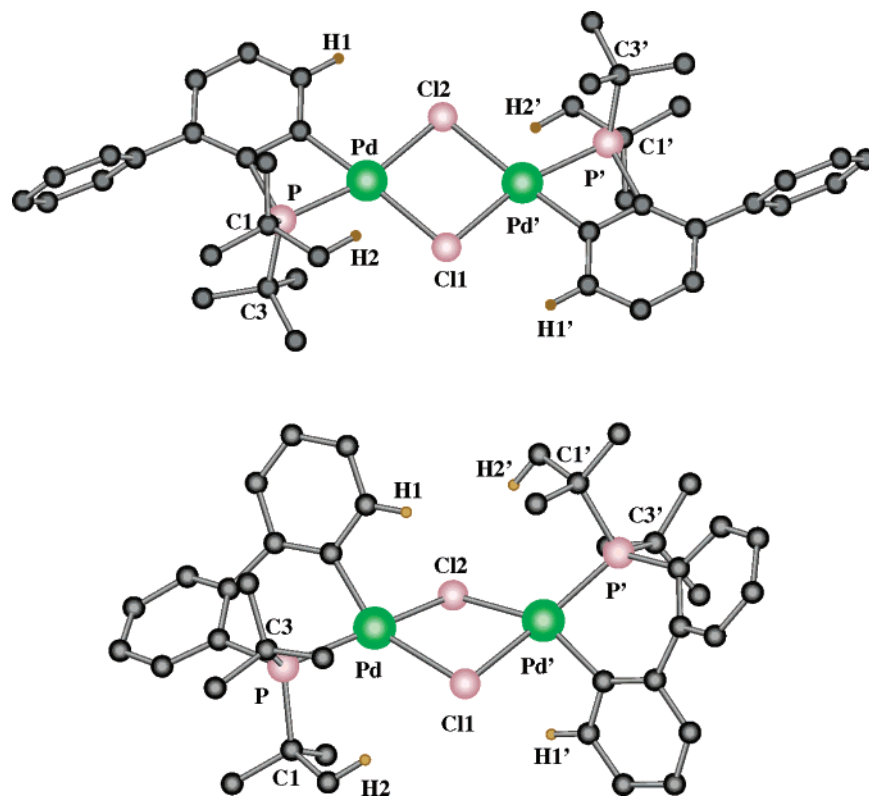


Figure 8. Computed structures for complexes **14-4r** (above) and **14-6r** (below). Nonsterically active hydrogen atoms are omitted for clarity.

the remote arene ring in **14-4r** is not constrained by coordination to the metal. As a result, it lies perpendicular to the P–C vector and avoids a destabilizing steric clash with the *tert*-butyl groups. In contrast, in **14-6r**, the remote arene ring is coordinated to the metal and, as a result, the *ortho* C–H group of the ring bonded to the phosphorus is forced to bisect the two *tert*-butyl groups. The result is a much more dramatic steric clash, causing the P–C bonds in **14-6r** to elongate—the average value is 1.895 Å compared to 1.872 Å in **14-4r**, and a lengthening of 0.023 Å is energetically significant for a strong single bond such as P–C. The repulsive Cl1–H2 contact is also closer in **14-6r** (ca. 2.80 Å) than in **14-4r** (ca. 3.06 Å). Entropic effects further tilt the balance in favor of **14-4r** because, unlike **14-6r**, it retains a freely rotating C–C single bond. Explicit calculation of the entropies of the two species suggests that this contributes a further 4 kcal/mol in favor of **14-4r**, bringing it below **14-6r** on the free-energy surface.

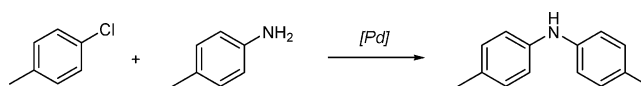
Catalytic Amination of Aryl Halides Using Dipalladium Compounds 2–5 as Precatalysts. As stated in the Introduction, we reported in a preliminary communication that **2** and **3** are effective precatalysts for the amination of aryl bromides and chlorides at room temperature. To study the catalytic properties of these compounds in more detail, the model reaction shown in Scheme 6 was carried out using different dipalladium compounds as precatalysts. Since the dinuclear complex **6** is not particularly stable in solution, we decided to study only complexes **2–5** and to compare their catalytic properties with the species generated by mixing Pd₂(dba)₃ with the corresponding phosphine. As can be seen in Table 1, the four complexes accelerate the reaction at room temperature and, particularly, in the case of **4** and **5**, in very short periods of time. To probe the rate of catalysis, the reaction with the dinuclear dimer **4** (at 0.5 mol %) was monitored over time (Figure 9). More than

Table 1. Catalytic Amination of 4-Chlorotoluene with *p*-Toluidine (see Scheme 6) Using Different Palladium Sources^a

entry	precatalyst	[mol % Pd]	T	Conversion (%) ^b at Different Times (h)				
				0.5	1	2	3	24
1	2	1	rt	21	38	45	75	100
2	2	2	rt	50	66	86	93	100
3	3	1	rt	29	48	63	75	99
4	3	2	rt	59	70	86	91	100
5	4	1	rt	82	92	96	99	100
6	4	2	rt	91	96	99	100	
7	5	1	rt	92	93	97	99	100
8	5	2	rt	95	98	100		
9	Pd ₂ dba ₃ /P ^t Bu ₂ Bph	1	rt			4 ^c	7	10
10	Pd ₂ dba ₃ /P ^t Bu ₂ Bph	0.5	80 °C			90 ^d		
11	Pd ₂ dba ₃ /P ^t Bu ₂ Bph(Me)	1	rt			4 ^e	4	6
12	Pd ₂ dba ₃ /P ^t Bu ₂ Bph(Me)	1	80 °C	58	88	99 ^e		

^a Conditions: 1.0 equiv of aryl chloride, 1.2 equiv amine, 1.4 equiv of NaO^tBu, THF (1.2 mL/mmol aryl chloride). ^b GC conversion of aryl chloride (see Scheme 4), average of at least two runs. The conversion of this aryl chloride to the corresponding coupled product is very clean with no other products being formed; consequently, the GC % conversion (instead of GC % yield) is a good measure of the catalytic activity of the complexes. ^c Ratio L/Pd of 1:1, in toluene (2 mL/mmol aryl chloride). ^d Ratio L/Pd of 1:1, in toluene (2 mL/mmol aryl chloride), 2.5 h, isolated yield.⁶⁴ ^e Ratio L/Pd of 2:1, in toluene (2 mL/mmol aryl chloride).

Scheme 6



60% conversion was reached within the first 5 min, and after 20 min, more than 80% of the product was obtained. Although these are preliminary investigations, the results presented in Figure 9 show that the activation of the catalyst occurs readily since high yields of the cross-coupling product are produced within the first few minutes of reaction. Interestingly, when the

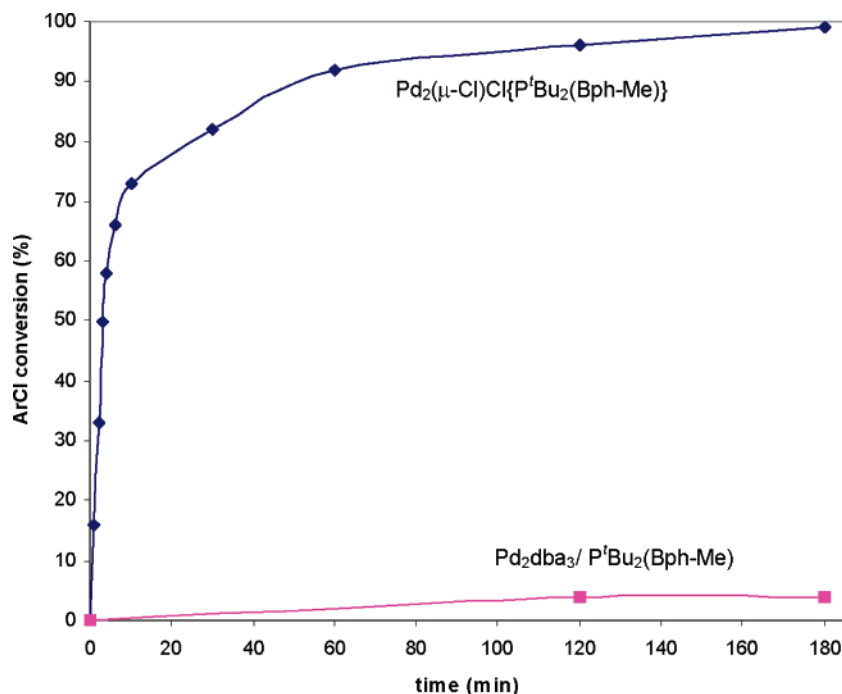


Figure 9. Plot of % conversion versus time for the reaction in toluene of 4-chlorotoluene with *p*-toluidine at room temperature in the presence of **4** and a Pd₂(dba)₃/P^tBu₂(Bph-Me) mixture. The amount of compound added in each case was such that a 1 mol % of palladium was present in the solution.

reaction between Pd₂(dba)₃ and P^tBu₂(Bph-Me) (the same phosphine present in **4**) was monitored at room temperature, the cross-coupling yields were very low even after 2 h (see Table 1 and Figure 9). Only when this reaction was warmed to 80 °C in toluene were the yields comparable to the systems catalyzed by the dinuclear compound. This apparent slower rate of reaction for the mixture Pd₂(dba)₃/P^tBu₂(Bph-Me) in comparison to the corresponding dimer **4** may simply be a consequence of the slow reaction of Pd₂(dba)₃ with bulky biphenyl phosphines at room temperature. Hence, the rate-limiting step of the reaction with Pd₂(dba)₃/P^tBu₂(Bph-Me) is most probably the formation of the catalytically active species.

To confirm that the catalytic activity of these systems was not due to one of the “decomposition” products (e.g., the cyclometalated compound), the above reaction was investigated in the presence of compound **14** as a potential catalyst. Using analogous experimental conditions to the ones described above (1% mol catalyst, i.e., 2% palladium loading, in THF and at room temperature), no coupling product was detected with this palladium(II) compound after 4 h. This indicates that the high activity of the aryl-bridged dimers **2–5** is not due to the corresponding cyclometalated compound.

Once it was established that the biaryl-bridged dimers (specially **4** and **5**) are effective precatalysts for the coupling of 4-chlorotoluene with *p*-toluidine, it was of interest to investigate the scope of these compounds for the catalysis of other—more challenging—substrates. Thus, the coupling of a range of substrate combinations (see Table 2) was investigated using compound **4** as a precatalyst. This dimer was chosen as it can be synthesized in high yields and is not air-sensitive (hence it can be weighed out and handled in air). Table 2 summarizes the results of these amination reactions. As can be seen from entries 2, 3, and 5, it is possible to use a cyclic secondary aliphatic amine (namely, morpholine) as substrate in the amination reaction. The isolated yields of the corresponding

products are above 93% for the coupling of this amine with *para*-substituted aryl chlorides (entries 2 and 5), even when the substituent is an electron-donating group, such as methoxy. The usually difficult coupling of morpholine with an *ortho*-substituted aryl chloride (entry 3) gave the corresponding product in 85% yield using 2 mol % of palladium. Excellent yields (95%) are obtained when the *ortho*-substituted 2-chlorotoluene is coupled with benzylamine at room temperature within 1 h.

The coupling of 4-chlorotoluene with benzylamine was also investigated, giving 76% conversion of the aryl chloride within 1 h (using 1 mol % of Pd). However, the reaction gave both the mono- and bisarylated products in a 5:1 ratio. Due to the relatively low conversion (in comparison to the other reactions) and the formation of more than one product, only the GC conversion was recorded and no further treatment of the mixture was carried out (and hence this entry is not shown in Table 2).

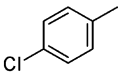
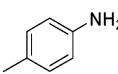
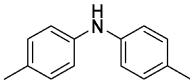
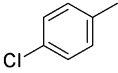
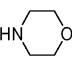
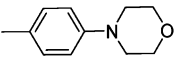
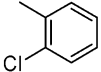
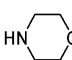
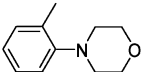
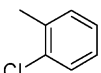
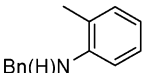
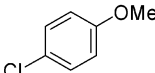
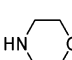
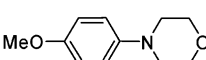
This preliminary screening indicates that **4** is an effective precatalyst for the room temperature amination of both electron-deficient and electron-rich aryl chlorides. Furthermore, we have shown that the system is compatible with both aliphatic and aromatic amines (primary and secondary). To the best of our knowledge, the rates at which these reactions take place are considerably higher than those reported when a mixture of a palladium source and the corresponding phosphine is employed to generate the catalyst *in situ*.⁶⁴ We anticipate that even better yields and reaction rates will be achieved by optimizing the reaction conditions at which these dimers catalyze the amination of aryl chlorides.

Conclusions

A series of new dinuclear palladium species with a bridging aryl group have been prepared. These compounds have proved

(64) Wolfe, J. P.; Tomori, H.; Sadighi, J. P.; Yin, J.; Buchwald, S. L. *J. Org. Chem.* **2000**, *65*, 1158–1174.

Table 2. Room Temperature Amination of Aryl Chlorides^a

entry	halide	amine	product	%Pd	time(h)	yield (isolated) ^{b,c}
1				1	3	90%
2				1	1	93%
3				2	8	85%
4		H ₂ NBn		1	1	95%
5				1	4	90%

^a Reaction conditions: 1.0 equiv of aryl chloride, 1.2 equiv of amine, 1.4 equiv of NaOtBu, 0.5–1 mol % of Pd₂(μ-Cl)Cl(P'Bu₂Bph-Me) (**4**), THF (1.1 mL/mmol aryl chloride, rt). ^b Isolated yields (average of two runs). ^c The spectroscopic data for the isolated products were identical to those reported before.^{65,66}

to be excellent precatalysts for the room temperature amination of aryl chlorides (including *ortho*-substituted and electron-rich). Crystal structures of the dinuclear and mononuclear species initially suggested highly unusual and symmetric $\eta^3:\eta^3$ and η^1 arene coordination modes, respectively. Density functional theory has, however, failed to locate minima corresponding to these structures and suggests instead that the coordination modes are better described as distorted $\eta^2:\eta^2$ and η^2 , respectively. The observed crystal structures are therefore most likely to be a result of crystallographic disorder between isomers with very similar energies. The high degree of coordinative flexibility shown by the arene ring of the biphenyl group may have important implications in the catalytic cycle, where it could act as an electronic buffer. The aryl-bridged dinuclear palladium compounds dissociate in solution, yielding palladium(II) monophosphine complexes which, in some cases, decompose to form dinuclear cyclometalated products containing unusual four-membered metallacycles. In the absence of the *tert*-Bu groups, calculations indicate that the thermodynamic product should feature six- rather than four-membered rings. The inclusion of the phosphine substituents in the computational model, however, reverses this preference by destabilizing the more crowded six-membered product. This offers clear evidence for the important role of steric bulk of the phosphine. The overall reaction chemistry, and presumably catalytic efficiency, of these systems therefore depends critically on both the electronic and steric properties of the phosphine ligand, as well as solvent and temperature.

Experimental Section

General. All experimental procedures were carried out using standard high vacuum and Schlenk line techniques under an atmosphere of dry argon. Glassware was dried in an oven at 150 °C prior to use. CH₂Cl₂, hexane, THF, methanol, diethyl ether, and toluene were dried using a solvent purification system (SPS, Innovative Technology) and degassed with argon prior to use. ¹H, ¹³C, and ³¹P NMR spectra were recorded on a Bruker Avance 400 or Bruker Avance 500 spectrometer and referenced to residual ¹H and ¹³C signals of the solvents or 85% H₃PO₄ as an external standard (³¹P). Elemental analyses were carried out at the Universidad de Santiago de Compostela. ESI-MS and MALDI spectra were obtained by J. Barr at the Institute of Chemical Research of Catalonia (ICIQ). GC-MS were recorded on an Agilent Technology 6890N gas chromatographer equipped with an Agilent-5973 Mass Selective Detector using a HP-5 methyl silicone column. The following compounds, Pd(COD)Br₂,⁶⁷ Pd(COD)Cl₂,⁶⁷ [Pd₂(dba)₃]·C₆H₆,⁶⁸ Pd₂(μ-Br)Br{μ-P'Bu₂(Bph-H)},⁴⁹ and Pd₂(μ-Cl)Cl{μ-P'Bu₂(Bph-H)},⁴⁹ were synthesized following literature procedures. The phosphines, P'Bu₂(Bph-H), P'Bu₂(Bph-Me), and P'Bu₂(Bph-NMe₂), were purchased from Strem chemicals. The NMR assignments were confirmed by ¹H COSY, ¹H NOESY, HSQC (¹H–¹³C), and HMBC (¹H–¹³C) experiments. The numbering scheme for NMR assignments is shown in Figures 10 and 11.

Synthesis of Pd₂(μ-Cl)Cl{μ-P'Bu₂(Bph-H)} (2**).** This compound was prepared according to the method we previously reported in a

(65) Wolfe, J. P.; Buchwald, S. L. *J. Am. Chem. Soc.* **1997**, *119*, 6054–6058.

(66) Kataoka, N.; Shelby, Q.; Stambuli, J. P.; Hartwig, J. F. *J. Org. Chem.* **2002**, *67*, 5553–5566.

(67) Drew, D.; Doyle, J. R. *Inorg. Synth.* **1990**, *28*, 346–349.

(68) Ukai, T.; Kawazura, H.; Ishii, Y.; Bonnet, J. J.; Ibers, J. A. *J. Organomet. Chem.* **1974**, *65*, 253–266.

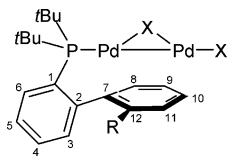


Figure 10. Numbering scheme for the NMR assignments of compounds 2–6.

preliminary communication. The complete and detailed NMR assignments are herein reported. ^1H NMR (400 MHz, CD_2Cl_2): δ 7.78–7.73 (m, H-6), 7.63–7.58 (m, H-4), 7.56–7.50 (m, H-5), 7.34–7.30 (m, H-3), 6.63–6.58 (m, H-10), 6.47–6.41 (m, H-9, H-11), 6.05–6.01 (m, H-8, H-12), 1.36 (d, 18H, $^3J_{\text{PH}} = 14.9$ Hz, $\text{C}(\text{CH}_3)_3$). $^{13}\text{C}\{^1\text{H}\}$ NMR (126 MHz, CD_2Cl_2): δ 146.9 (d, $J_{\text{PC}} = 19.8$ Hz, C-2), 136.9 (d, $J_{\text{PC}} = 32.8$ Hz, C-1), 133.7 (d, $J_{\text{PC}} = 1.7$ Hz, C-6), 132.6 (d, $J_{\text{PC}} = 19.0$ Hz, C-3), 132.5 (d, $J_{\text{PC}} = 4.3$ Hz, C-4), 129.1 (d, $J_{\text{PC}} = 4.7$ Hz, C-5), 110.0 (d, $J_{\text{PC}} = 3.9$ Hz, C-8, C-12), 107.8 (d, $J_{\text{PC}} = 3.5$ Hz, C-9, C-11), 105.0 (d, $J_{\text{PC}} = 6.9$ Hz, C-7), 69.9 (d, $J_{\text{PC}} = 1.3$ Hz, C-10), 36.3 (d, $J_{\text{PC}} = 11.5$ Hz, $\text{C}(\text{CH}_3)_3$), 30.0 (d, $J_{\text{PC}} = 5.4$ Hz, $\text{C}(\text{CH}_3)_3$).

Synthesis of $\text{Pd}_2(\mu\text{-Cl})\text{Cl}\{\mu\text{-P}^t\text{Bu}_2(\text{Bph-Me})\}$ (4). A toluene solution (10 mL) of $\text{Pd}_2\text{dba}_3\cdot\text{C}_6\text{H}_6$ (128 mg, 0.128 mmol) and $\text{P}^t\text{Bu}_2(\text{Bph-Me})$ (80 mg, 0.257 mmol) was stirred for 18 h. To the resulting orange-red solution was added $\text{Pd}(\text{COD})\text{Cl}_2$ (67 mg, 0.257 mmol), and the reaction mixture was stirred for further 15 h after which time a dark solid precipitated. The reaction mixture was filtered and the solid residue washed with diethyl ether (3×5 mL). The crude product was purified by flash column chromatography ($\text{CH}_2\text{Cl}_2/\text{CH}_3\text{OH}$ 9:1) on silica gel to give 4 as dark-green solid. Yield: 114 mg (74%). ^1H NMR (400 MHz, CD_2Cl_2): δ 7.80–7.75 (m, H-6), 7.65–7.60 (m, H-4), 7.56–7.50 (m, H-5), 7.30 (d, $^3J_{\text{HH}} = 7.92$ Hz, H-3), 6.62–6.57 (m, H-10), 6.44 (d, $^3J_{\text{HH}} = 6.20$ Hz, H-11), 6.32–6.27 (m, H-9), 5.86 (d, $^3J_{\text{HH}} = 7.60$ Hz, H-8), 1.71 (s, 3H, Me), 1.40 (d, 9H, $^3J_{\text{PH}} = 14.9$ Hz, $\text{C}(\text{CH}_3)_3$), 1.33 (d, 9H, $^3J_{\text{PH}} = 14.5$ Hz, $\text{C}(\text{CH}_3)_3$). $^{13}\text{C}\{^1\text{H}\}$ NMR (126 MHz, CD_2Cl_2): δ 146.9 (C-7), 138.1 (d, $J_{\text{PC}} = 30.27$ Hz, C-1), 134.4 (C-6), 132.9 (d, $J_{\text{PC}} = 1.89$ Hz, C-4), 132.8 (d, $J_{\text{PC}} = 16.62$ Hz, C-3), 129.1 (d, $J_{\text{PC}} = 4.92$ Hz, C-5), 128.8 (d, $J_{\text{PC}} = 3.99$ Hz, C-12), 112.7 (d, $J_{\text{PC}} = 2.72$ Hz, C-11), 107.1 (d, $J_{\text{PC}} = 3.99$ Hz, C-2), 106.2 (d, $J_{\text{PC}} = 3.83$ Hz, C-8), 105.2 (d, $J_{\text{PC}} = 2.35$ Hz, C-9), 71.2 (C-10), 37.1 (d, $J_{\text{PC}} = 12.0$ Hz, $\text{C}(\text{CH}_3)_3$), 36.7 (d, $J_{\text{PC}} = 12.0$ Hz, $\text{C}(\text{CH}_3)_3$), 30.8 (d, $J_{\text{PC}} = 5.6$ Hz, $\text{C}(\text{CH}_3)_3$), 30.7 (d, $J_{\text{PC}} = 5.5$ Hz, $\text{C}(\text{CH}_3)_3$), 21.0 (Me). $^{31}\text{P}\{^1\text{H}\}$ NMR (202 MHz, CD_2Cl_2): δ 62.1 (s). HRMS-ESI calcd for $\text{C}_{23}\text{H}_{32}\text{ClNPPd}_2$ ($\text{M}^+ + \text{MeCN} - \text{Cl}$): 602.0035. Found: 602.0068. Anal. Calcd for $\text{C}_{21}\text{H}_{29}\text{Cl}_2\text{PPd}_2$: C, 42.31; H, 4.90. Found: C, 42.34; H, 5.22.

Synthesis of $\text{Pd}_2(\mu\text{-Br})\text{Br}\{\mu\text{-P}^t\text{Bu}_2(\text{Bph-Me})\}$ (5). A toluene solution (8 mL) of $\text{Pd}_2\text{dba}_3\cdot\text{C}_6\text{H}_6$ (103 mg, 0.103 mmol) and $\text{P}^t\text{Bu}_2(\text{Bph-Me})$ (64 mg, 0.207 mmol) was stirred for 18 h. To the resulting orange-red solution was added $\text{Pd}(\text{COD})\text{Br}_2$ (62 mg, 0.165 mmol), and the reaction mixture was stirred for further 5 h after which time a dark solid precipitated. The reaction mixture was filtered and the brown solid residue washed with diethyl ether (3×3 mL). The crude solid was extracted with THF (3×3 mL), and the combined THF fractions were concentrated. After the addition of hexane, a dark solid precipitated; this was isolated by filtration and dried under reduced pressure. Yield: 30 mg (26%). ^1H NMR (500 MHz, $\text{THF}-d_8$): δ 7.96–7.90 (m, H-6), 7.68–7.65 (m, H-4), 7.59–7.56 (m, H-5), 7.43 (d, $^3J_{\text{HH}} = 7.90$ Hz, H-3), 6.91–6.87 (m, H-10), 6.50 (d, $^3J_{\text{HH}} = 5.70$ Hz, H-11), 6.29–6.24 (m, H-9), 6.01 (d, $^3J_{\text{HH}} = 7.60$ Hz, H-8), 1.70 (s, 3H, Me), 1.41 (d, 9H, $^3J_{\text{PH}} = 15.0$ Hz, $\text{C}(\text{CH}_3)_3$), 1.35 (d, 9H, $^3J_{\text{PH}} = 14.5$ Hz, $\text{C}(\text{CH}_3)_3$). $^{31}\text{P}\{^1\text{H}\}$ NMR (202 MHz, $\text{THF}-d_8$): δ 67.9 (s). HRMS-ESI calcd for $\text{C}_{23}\text{H}_{32}\text{BrNPPd}_2$ ($\text{M}^+ + \text{MeCN} - \text{Br}$): 645.9529. Found: 645.9541. Anal. Calcd for $\text{C}_{21}\text{H}_{29}\text{Br}_2\text{PPd}_2$: C, 36.82; H, 4.27. Found: C, 36.41; H, 3.97.

Synthesis of $\text{Pd}_2(\mu\text{-Cl})\text{Cl}\{\mu\text{-P}^t\text{Bu}_2(\text{Bph-NMe}_2)\}$ (6). A toluene solution (10 mL) of $\text{Pd}_2\text{dba}_3\cdot\text{C}_6\text{H}_6$ (0.150 g, 0.150 mmol) and $\text{P}^t\text{Bu}_2\text{-Bph-NMe}_2$ (0.103 g, 0.301 mmol) was stirred for 48 h. To the resulting red solution was added $\text{Pd}(\text{COD})\text{Cl}_2$, and the reaction mixture was

stirred for further 5 h after which time a dark solid precipitated. The reaction mixture was filtered to isolate the solid product, and from the filtrate, crystals grew overnight. The solvent was removed via cannula, and the crystals were washed with diethyl ether (3×3 mL) and dried under vacuum. The crystalline material was analyzed by X-ray crystallography and by ^1H and $^{31}\text{P}\{^1\text{H}\}$ spectroscopy. ^1H NMR (CD_2Cl_2 , 500 MHz): δ 7.80–7.74 (m, 1H), 7.65–7.59 (m, 1H), 7.56–7.46 (m, 2H), 6.50–6.45 (m, 1H), 6.09–5.98 (m, 2H), 5.87 (d, $^3J_{\text{HH}} = 7.6$ Hz, 1H), 2.34 (s, 3H, Me), 1.44 (d, 9H, $^3J_{\text{PH}} = 15.0$ Hz, $\text{C}(\text{CH}_3)_3$), 1.24 (d, 9H, $^3J_{\text{PH}} = 14.9$ Hz, $\text{C}(\text{CH}_3)_3$). $^{31}\text{P}\{^1\text{H}\}$ NMR (CD_2Cl_2 , 202 MHz): δ 63.6 (s).

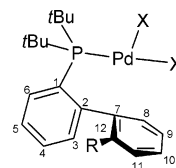


Figure 11. Numbering scheme for the NMR assignments of compounds 8–10.

Synthesis of $\text{Pd}(\text{Br})_2\{\eta^1\text{-P}^t\text{Bu}_2(\text{Bph-NMe}_2)\}$ (8). Method A: A Schlenk flask was charged with $\text{Pd}_2\text{dba}_3\cdot\text{C}_6\text{H}_6$ (148 mg, 0.148 mmol) and $\text{P}^t\text{Bu}_2(\text{Bph-NMe}_2)$ (101 mg, 0.298 mmol), evacuated, and backfilled with argon. Toluene (10 mL) was added, and the resulting reaction mixture was stirred for 48 h. After this time, $\text{Pd}(\text{COD})\text{Br}_2$ (111 mg, 0.297 mmol) was added as a solid. After 1 h, a dark solid precipitated (together with the formation of palladium metal on the walls of the reaction vessel). The solution was filtered and the solid washed with diethyl ether (3×3 mL). The residue was extracted with CH_2Cl_2 , the combined washings were concentrated, and hexane was added to precipitate a dark blue solid. The solution was filtered, and the crude solid was purified by column chromatography on silica gel ($\text{CH}_2\text{Cl}_2 \rightarrow \text{CH}_2\text{Cl}_2/\text{MeOH}$ 10:1). Yield: 75 mg (42%). Single crystals suitable for X-ray crystallography were obtained by slow evaporation of a saturated dichloromethane solution of 8. ^1H NMR (400 MHz, CD_2Cl_2): δ 7.84–7.78 (m, H-6), 7.68–7.57 (m, H-10), 7.38–7.20 (m, H-4, H-5, H-8), 7.02 (d, $^3J_{\text{HH}} = 8.80$ Hz, H-11), 6.71 (d, $^3J_{\text{HH}} = 7.45$ Hz, H-3), 6.55 (dd, $^3J_{\text{HH}} = \text{ca. } 7.44$, $\text{ca. } 7.44$ Hz, H-9), 3.25 (s, NMe_2), 1.74 (d, 9H, $^3J_{\text{PH}} = 14.3$ Hz, $\text{C}(\text{CH}_3)_3$), 1.65 (d, 9H, $^3J_{\text{PH}} = 14.9$ Hz, $\text{C}(\text{CH}_3)_3$). $^{31}\text{P}\{^1\text{H}\}$ NMR (CD_2Cl_2 , 202 MHz): δ 77.8 (s). HRMS-ESI calcd for $\text{C}_{22}\text{H}_{32}\text{BrNPPd}$ ($\text{M}^+ - \text{Br}$): 526.0494. Found: 526.0429.

Method B: The phosphine $\text{P}^t\text{Bu}_2\text{Bph}(\text{NMe}_2)$ (93 mg, 0.275 mmol) and $\text{Pd}(\text{COD})\text{Br}_2$ (103 mg, 0.275 mmol) were dissolved in CH_2Cl_2 (6 mL). The reaction mixture was stirred for 7 h, and after this time, the solvent was removed under reduced pressure. The residue was washed with diethyl ether (3×6 mL). The crude product was purified on a silica gel column ($\text{CH}_2\text{Cl}_2 \rightarrow \text{CH}_2\text{Cl}_2/\text{MeOH}$ 10:1) to obtain a black-blue solid. Yield: 85 mg (51%). ^1H NMR (400 MHz, CD_2Cl_2): δ 7.84–7.79 (m, H-6), 7.65–7.59 (m, H-10), 7.34–7.24 (m, H-4, H-5, H-8), 7.02 (d, $^3J_{\text{HH}} = 8.76$ Hz, H-11), 6.73–6.69 (m, H-3), 6.55 (dd, $^3J_{\text{HH}} = 7.80$, 7.02 Hz), 3.25 (s, NMe_2), 1.75 (d, 9H, $^3J_{\text{PH}} = 14.3$ Hz, $\text{C}(\text{CH}_3)_3$), 1.64 (d, 9H, $^3J_{\text{PH}} = 15.0$ Hz, $\text{C}(\text{CH}_3)_3$). $^{31}\text{P}\{^1\text{H}\}$ NMR (202 MHz, CD_2Cl_2): δ 77.9 (s). Anal. Calcd for $\text{C}_{22}\text{H}_{32}\text{Br}_2\text{NPPd}$: C, 43.48; H, 5.31; N, 2.30. Found: C, 43.22; H, 5.12; N, 2.24.

Synthesis of $\text{Pd}(\text{Cl})_2\{\eta^1\text{-P}^t\text{Bu}_2(\text{Bph-NMe}_2)\}$ (9). Method A: A Schlenk flask was charged with $\text{Pd}_2\text{dba}_3\cdot\text{C}_6\text{H}_6$ (84 mg, 0.084 mmol) and $\text{P}^t\text{Bu}_2(\text{Bph-NMe}_2)$ (57 mg, 0.169 mmol), evacuated, and backfilled with argon. Then toluene (6 mL) was added. The reaction mixture was stirred for 48 h. To the red-orange solution was added $\text{Pd}(\text{COD})\text{Cl}_2$ (36 mg, 0.127 mmol). The reaction solution was stirred for further 8 h. The solution was filtered and the residue washed with diethyl ether (3×3 mL). The crude product was purified by flash column chromatography on silica gel ($\text{CH}_2\text{Cl}_2 \rightarrow \text{CH}_2\text{Cl}_2/\text{MeOH}$ 10:1). Yield: 49 mg (73%, related to used amounts of $\text{Pd}(\text{COD})\text{Cl}_2$). ^1H NMR (400 MHz, CD_2Cl_2): δ 7.81–7.76 (m, H-6), 7.72–7.66 (ddd, $^3J_{\text{HH}} = 9.2$,

6.56 Hz, $^4J_{\text{HH}} = 1.28$ Hz, H-10), 7.35–7.26 (m, H-4, H-5, H-8), 6.93 (d, $^3J_{\text{HH}} = 8.72$ Hz, H-11), 6.76–6.69 (m, H-3), 6.54 (dd, $^3J_{\text{HH}} = 7.36$, 7.36 Hz, H-9), 3.28 (s, NMe_2), 1.71 (d, 9H, $^3J_{\text{PH}} = 14.5$ Hz, $\text{C}(\text{CH}_3)_3$), 1.66 (d, 9H, $^3J_{\text{PH}} = 15.0$ Hz, $\text{C}(\text{CH}_3)_3$). $^{31}\text{P}\{^1\text{H}\}$ NMR (162 MHz, CD_2Cl_2): δ 76.9 (s). MALDI(+)-MS: m/z 484 [$\text{M}^+ - \text{Cl}$]. **Method B:** The phosphine $\text{P}^i\text{Bu}_2\text{Bph}(\text{NMe}_2)$ (47 mg, 0.136 mmol) and $\text{Pd}(\text{COD})\text{-Cl}_2$ (39 mg, 0.136 mmol) were dissolved in CH_2Cl_2 (5 mL). The solution turned purple after 30 min. After 6 h, all phosphine has been consumed (as judged by in situ $^{31}\text{P}\{^1\text{H}\}$ NMR), and the solvent was removed under reduced pressure. The residue was washed with diethyl ether (2×5 mL) and dried under vacuum to obtain **9** as a purple powder. Yield: 63 mg (89%). ^1H NMR (400 MHz, CD_2Cl_2): δ 7.81–7.76 (m, H-6), 7.69 (ddd, $^3J_{\text{HH}} = 8.75$, 6.98 Hz, $^4J_{\text{HH}} = 1.50$ Hz, H-10), 7.34–7.25 (m, H-4, H-5, H-8), 6.94 (d, $^3J_{\text{HH}} = 8.75$ Hz, H-11), 6.74–6.70 (m, H-3), 6.54 (dd, $^3J_{\text{HH}} = 7.50$, 7.05 Hz, H-9), 3.28 (s, NMe_2), 1.71 (d, 9H, $^3J_{\text{PH}} = 15.2$ Hz, $\text{C}(\text{CH}_3)_3$), 1.66 (d, 9H, $^3J_{\text{PH}} = 14.4$ Hz, $\text{C}(\text{CH}_3)_3$). $^{13}\text{C}\{^1\text{H}\}$ NMR (100 MHz, CDCl_3): δ 167.9 (C-12), 152.3 (d, $J_{\text{PC}} = 15.4$ Hz, C-2), 142.5 (C-10), 135.9 (C-6), 132.3 (d, $J_{\text{PC}} = 1.97$ Hz, C-arom.), 130.6 (d, $J_{\text{PC}} = 14.82$ Hz, C-3), 130.3 (C-1), 130.1 (d, $J_{\text{PC}} = 1.48$ Hz, C-arom.), 126.4 (d, $J_{\text{PC}} = 5.71$ Hz, C-arom.), 116.4 (C-11), 115.0 (C-9), 86.5 (C-7), 45.5 ($\text{N}(\text{CH}_3)_2$), 41.8 ($\text{C}(\text{CH}_3)_3$), 41.3 (d, $J_{\text{PC}} = 7.32$ Hz, $\text{C}(\text{CH}_3)_3$), 32.0 (d, $J_{\text{PC}} = 2.25$ Hz, $\text{C}(\text{CH}_3)_3$), 31.90 (d, $J_{\text{PC}} = 2.90$ Hz, $\text{C}(\text{CH}_3)_3$). $^{31}\text{P}\{^1\text{H}\}$ NMR (162 MHz, CD_2Cl_2): δ 76.9 (s). MALDI(+)-MS: m/z 484 [$\text{M}^+ - \text{Cl}$]. Anal. Calcd for $\text{C}_{22}\text{H}_{32}\text{-Cl}_2\text{NPPd}$: C, 50.93; H, 6.22; N, 2.70. Found: C, 50.94; H, 6.08; N, 2.63.

Synthesis of $\text{Pd}(\text{Cl})_2[\eta^1\text{-P}^i\text{Bu}_2(\text{Bph-Me})]$ (10**).** In a glovebox, the phosphine (96 mg, 0.3082 mmol) and $\text{Pd}(\text{COD})\text{Cl}_2$ (80 mg, 0.280 mmol) were weighed and transferred to Schlenk. The Schlenk was removed from the glovebox, and CH_2Cl_2 (3 mL) was added. After the reaction was stirred for 2.5 h, the solvent was removed under reduced pressure. The obtained orange oil was broken by the addition of hexane and filtered. This procedure was repeated three times in total to yield a red-brown powder. The crude product was purified by column chromatography on silica gel ($\text{CH}_2\text{Cl}_2/\text{MeOH}$ 20:1). Yield: 112 mg (81%). ^1H NMR (400 MHz, CD_2Cl_2): δ 7.89–7.82 (m, 2H), 7.53–7.33 (m, 4H), 6.95 (d, $^3J_{\text{HH}} = 7.36$ Hz, 1H), 6.81 (d, $^3J_{\text{HH}} = 7.20$ Hz, 1H), 2.50 (s, Me), 1.70 (d, 9H, $^3J_{\text{PH}} = 15.0$ Hz, $\text{C}(\text{CH}_3)_3$), 1.65 (d, 9H, $^3J_{\text{PH}} = 15.0$ Hz, $\text{C}(\text{CH}_3)_3$). $^{31}\text{P}\{^1\text{H}\}$ NMR (162 MHz, CD_2Cl_2): δ 75.6 (s). ESI-MS: m/z^+ 455 ($\text{M}^+ - \text{Cl}$). Elemental analyses for this compound are not provided due to the presence of traces of the cyclometalated product **14** (see below) detected by $^{31}\text{P}\{^1\text{H}\}$ NMR spectroscopy.

Synthesis of Palladacycle **14.** $\text{Pd}(\text{COD})\text{Cl}_2$ (59 mg, 0.206 mmol) and $\text{P}^i\text{Bu}_2\text{Bph}(\text{Me})$ (65 mg, 0.208 mmol) were dissolved in CH_2Cl_2 (3 mL), and the reaction solution was stirred for 3 days at room temperature after which time a white precipitate had formed. The solvent was removed under reduced pressure. The crude product was purified by flash column chromatography on silica gel ($\text{CH}_2\text{Cl}_2/\text{hexane}$ 6:1). The obtained product was washed once with cold hexane and dried under vacuum to give an off-white solid. Yield: 40 mg (42%). Crystals suitable for X-ray diffraction studies were grown from a chloroform/hexane mixture. ^1H NMR (500 MHz, THF-d_8): δ 7.67–7.01 (m, 12H), 6.89 (dd, $J = 7.6$, 3.1 Hz, 2H), 2.11 (s, 6H, Me), 1.32 (br s, 36H, $\text{C}(\text{CH}_3)_3$). $^{13}\text{C}\{^1\text{H}\}$ NMR (126 MHz, THF-d_8): δ 143.0 (C-arom.), 142.2 (d, $J_{\text{PC}} = 4.3$ Hz, C-arom.), 140.2 (d, $J_{\text{PC}} = 34.2$ Hz, C-arom.), 137.3 (C-arom.), 136.3 (d, $J_{\text{PC}} = 24.9$ Hz, C-arom.), 131.1 (C-arom.), 130.5 (C-arom.), 130.1 (d, $J_{\text{PC}} = 4.7$ Hz, C-arom.), 129.5 (C-arom.), 129.0 (C-arom.), 128.6 (d, $J_{\text{PC}} = 9.1$ Hz, C-arom.), 125.8 (C-arom.), 36.7 (d, $J_{\text{PC}} = 12.6$ Hz, $\text{C}(\text{CH}_3)_3$), 30.8 (br s, $\text{C}(\text{CH}_3)_3$), 20.8 (s, Me, 6H). $^{31}\text{P}\{^1\text{H}\}$ NMR (162 MHz, THF-d_8): δ –13.1 (s). Anal. Calcd for $\text{C}_{42}\text{H}_{56}\text{Cl}_2\text{P}_2\text{-Pd}_2\text{H}_2\text{O}$: C, 54.56; H, 6.32. Found: C, 54.45; H, 6.45.

General Procedure for the Amination of 4-Chlorotoluene with *p*-Toluidine. The corresponding precatalyst (**2–5**) was weighed out in air and transferred to an oven-dried Schlenk. The Schlenk flask was evacuated and backfilled with argon, then NaO^tBu (1.4 mmol) and

p-toluidine (1.2 mmol) were added. This was followed by the addition of the aryl chloride (1 mmol) and THF (1.2 mL/mmol aryl chloride). The reaction mixture was stirred (see Table 1 for details of reaction times), and the samples were taken with a syringe at different times, quenched with water, passed through a small alumina column, and analyzed by GC-MS. For data points below 30 min, a stock solution of aryl chloride in THF was used instead of adding the neat aryl chloride into the reaction. The formulation of the reaction product (i.e., di-*p*-tolylamine) was confirmed by spectroscopic analysis.⁶⁵

General Procedure for the Room Temperature Amination of Aryl Chlorides (Table 2). The precatalyst (**4** (1–2 mol % of Pd) was weighed out in air and transferred to an oven-dried Schlenk flask, which was evacuated and backfilled with argon. Then, NaO^tBu (1.4 mmol) was added, and the flask was evacuated and backfilled with argon again. The amine (1.2 mmol) and the aryl chloride (1 mmol) were added through a septum followed by the addition of THF (1 mL/mmol aryl chloride) (*p*-toluidine as a solid was added following the addition of NaO^tBu). The reaction was monitored by GC-MS, and after complete consumption of the aryl chloride or after a certain period of time (see Table 2 for details), the reaction mixture was quenched with water. The mixture was extracted with CH_2Cl_2 , the organic layer was dried over MgSO_4 and concentrated. The residue was purified by column chromatography on silica gel with ethyl acetate/hexane.

X-ray Structure Determination: Crystals of **6**, **8**, and **14** were obtained from toluene, CH_2Cl_2 (slow evaporation), and a mixture of $\text{CHCl}_3/\text{hexane}$, respectively. The measured crystals were prepared under inert conditions immersed in perfluoropolyether as protecting oil for manipulation. **Data Collection:** Measurements were made on a Bruker-Nonius diffractometer equipped with an APEX 2 4K CCD area detector, a FR591 rotating anode with MoK_α radiation, Montel mirrors as monochromator, and a Kryoflex low-temperature device ($T = -173$ °C). Full-sphere data collection was used with ω and φ scans. **Programs used:** Data collection Apex2 V. 1.0–22 (Bruker-Nonius 2004), data reduction SAINT + Version 6.22 (Bruker-Nonius 2001), and absorption correction SADABS V. 2.10 (2003). **Structure Solution and Refinement:** SHELXTL Version 6.10 (Sheldrick, 2000) was used.

Computational Details. All calculations were carried out with the Gaussian03 package.⁶⁹ Pure DFT calculations used the mPW1PW91 functional, a hybrid functional⁷⁰ with modified Perdew–Wang exchange and Perdew–Wang correlation.⁷¹ An effective core potential was used to represent the 28 innermost electrons of palladium, and the associated SDD basis set was used for its valence electrons.⁷² A valence double- ζ plus polarization 6-31G(d,p) basis set was used for all other atoms.^{73–75} Hybrid QM/MM calculations with the ONIOM method^{76,77} used the same DFT description for the QM region and the UFF force field for the MM region.⁷⁸ The nonbonded radius for chlorine was increased by 0.4 Å to account for its anionic character.⁷⁹ All geometry optimizations were full, with no restriction.

Acknowledgment. We thank EPSRC (U.K.) (GR/R74970/01 and GR/R74963/01) and the ICIQ Foundation (Spain) for financial support, and Johnson Matthey for a loan of PdCl_2 . Dr. Gabriel Gonzalez and Mr. Kerman Gómez are thanked for

(69) Frisch, M. J.; et al. *Gaussian 03*, revision c.02; Wallingford, CT, 2004.

(70) Adamo, C.; Barone, V. *J. Chem. Phys.* **1998**, *108*, 664–675.

(71) Perdew, J. P.; Burke, K.; Wang, Y. *Phys. Rev. B: Condens. Matter* **1996**, *54*, 16533–16539.

(72) Andrae, D.; Haeussermann, U.; Dolg, M.; Stoll, H.; Preuss, H. *Theor. Chim. Acta* **1990**, *77*, 123–141.

(73) Hehre, W. J.; Lathan, W. A. *J. Chem. Phys.* **1972**, *56*, 5255–5257.

(74) Hariharan, P. C.; Pople, J. A. *Theor. Chim. Acta* **1973**, *28*, 213–222.

(75) Francl, M. M.; Pietro, W. J.; Hehre, W. J.; Binkley, J. S.; Gordon, M. S.;

DeFrees, D. J.; Pople, J. A. *J. Chem. Phys.* **1982**, *77*, 3654–3665.

(76) Maseras, F.; Morokuma, K. *J. Comput. Chem.* **1995**, *16*, 1170–1179.

(77) Vreven, T.; Morokuma, K. *J. Comput. Chem.* **2000**, *21*, 1419–1432.

(78) Rappe, A. K.; Casewit, C. J.; Colwell, K. S.; Goddard, W. A., III; Skiff, W. M. *J. Am. Chem. Soc.* **1992**, *114*, 10024–10035.

(79) Ujaque, G.; Maseras, F.; Eisenstein, O. *Theor. Chem. Acc.* **1997**, *96*, 146–150.

their help with the NMR data. D.A.P.'s visit to ICIQ and his calculations in CESC/CEPBA were funded by the HPC-EUROPA project (RII3-CT-2003-506079), with the support of the European Community—Research Infrastructure Action under the FP6 “Structuring the European Research Area” Programme.

Supporting Information Available: Cartesian coordinates and absolute energies for all computed structures. Complete ref 69. Crystallographic data (CIF). The supplementary crystallographic

data for this paper can also be obtained free of charge via www.ccdc.cam.ac.uk/conts/retrieving.html (or from the Cambridge Crystallographic Data Centre, 12, Union Road, Cambridge CB2 1EZ, U.K.; fax +44 1223 336033 or e-mail deposit@ccdc.cam.ac.uk). This material is available free of charge via the Internet at <http://pubs.acs.org>.

JA057825Z